The Journal of Experimental Biology 204, 1099–1122 (2001)
Printed in Great Britain © The Company of Biologists Limited 2001
JEB3037

MECHANICS OF LIMB BONE LOADING DURING TERRESTRIAL LOCOMOTION IN THE GREEN IGUANA (*IGUANA IGUANA*) AND AMERICAN ALLIGATOR (*ALLIGATOR MISSISSIPPIENSIS*)

RICHARD W. BLOB[1,*] AND ANDREW A. BIEWENER[2]

[1]*Department of Zoology, Division of Fishes, Field Museum of Natural History, 1400 South Lake Shore Drive, Chicago, IL 60605, USA* and [2]*Concord Field Station, MCZ, Harvard University, Old Causeway Road, Bedford, MA 01730, USA*

*e-mail: rblob@fmnh.org

Accepted 8 December 2000; published on WWW 26 February 2001

Summary

In vivo **measurements of strain in the femur and tibia of *Iguana iguana* (Linnaeus) and *Alligator mississippiensis* (Daudin) have indicated three ways in which limb bone loading in these species differs from patterns observed in most birds and mammals: (i) the limb bones of *I. iguana* and *A. mississippiensis* experience substantial torsion, (ii) the limb bones of *I. iguana* and *A. mississippiensis* have higher safety factors than those of birds or mammals, and (iii) load magnitudes in the limb bones of *A. mississippiensis* do not decrease uniformly with the use of a more upright posture. To verify these patterns, and to evaluate the ground and muscle forces that produce them, we collected three-dimensional kinematic and ground reaction force data from subadult *I. iguana* and *A. mississippiensis* using a force platform and high-speed video. The results of these force/kinematic studies generally confirm the loading regimes inferred from *in vivo* strain measurements. The ground reaction force applies a torsional moment to the femur and tibia in both species; for the femur, this moment augments the moment applied by the caudofemoralis muscle, suggesting large torsional stresses. In most cases, safety factors in bending calculated from force/video data are lower than those determined from strain data, but are as high or higher than the safety factors of bird and mammal limb bones in bending. Finally, correlations between limb posture and calculated stress magnitudes in the femur of *I. iguana* confirm patterns observed during direct bone strain recordings from *A. mississippiensis*: in more upright steps, tensile stresses on the anterior cortex decrease, but peak compressive stresses on the dorsal cortex increase. Equilibrium analyses indicate that bone stress increases as posture becomes more upright in saurians because the ankle and knee extensor muscles exert greater forces during upright locomotion. If this pattern of increased bone stress with the use of a more upright posture is typical of taxa using non-parasagittal kinematics, then similar increases in load magnitudes were probably experienced by lineages that underwent evolutionary shifts to a non-sprawling posture. High limb bone safety factors and small body size in these lineages could have helped to accommodate such increases in limb bone stress.**

Key words: locomotion, biomechanics, kinematics, force platform, bone stress, safety factor, posture, evolution, Sauria, Crocodylia, Lepidosauria, lizard.

Introduction

The limb postures of terrestrial tetrapods span a continuum from sprawling to fully upright, in which the limbs are held lateral to or beneath the body, respectively (Jenkins, 1971a; Gatesy, 1991; Reilly and Elias, 1998). Such differences in limb posture frequently are correlated with differences in limb kinematics. For instance, kinematic studies of lizards (Brinkman, 1980a; Brinkman, 1981; Jayne and Irschick, 1999; Irschick and Jayne, 1999) and crocodilians (Brinkman, 1980b; Gatesy, 1991) have demonstrated that axial rotation of the femur can be substantial during non-parasagittal locomotion in these lineages. These patterns contrast with those of tetrapods that employ parasagittal or near-parasagittal kinematics, in which axial rotation of the limb bones is minimal (Jenkins, 1971a). Because the loads that a limb bone experiences correlate strongly with its orientation to the ground reaction force during stance (Biewener, 1983a; Biewener et al., 1983; Biewener et al., 1988), vertebrate limbs used in non-parasagittal and parasagittal locomotion could be exposed to very different loading regimes. Few studies have explicitly tested this possibility. However, such studies are necessary to evaluate the potential diversity of tetrapod limb bone loading patterns and to understand major aspects of evolutionary transitions in tetrapod locomotor mechanics.

Measurements of *in vivo* strain from the femur and tibia in

Iguana iguana and *Alligator mississippiensis* (Blob and Biewener, 1999) suggest that loading patterns in the limb bones of these species differ from those of previously examined terrestrial mammals and birds in two fundamental ways: (i) shear is a much more important mode of loading in *I. iguana* and *A. mississippiensis* than in most species that habitually use upright locomotion, and (ii) limb bone safety factors are higher in *I. iguana* and *A. mississippiensis* than in birds or mammals. Our data suggest a further distinction between *A. mississippiensis* and mammals: in contrast to interspecific patterns observed in mammals (Biewener, 1989; Biewener, 1990), bone loads did not decrease throughout the cortex when *A. mississippiensis* used more upright postures but, instead, increased at some locations (Blob and Biewener, 1999). Because limb bone loading mechanics have been examined in only two species that employ non-parasagittal locomotion, broad conclusions based on studies of *I. iguana* and *A. mississippiensis* must be viewed with caution. However, bone strain data from these species suggest preliminary hypotheses that substantial limb bone torsion, high limb bone safety factors, and increases in bone loading with the use of a more upright stance are common features of locomotor mechanics among tetrapods that use non-parasagittal kinematics and a non-upright limb posture.

As a first step in testing these hypotheses, we collected simultaneous three-dimensional kinematic and force platform data from iguanas and alligators. Integrated force and kinematic data provide an independent means of verifying the interpretations of load magnitudes and loading patterns derived from bone strain recordings. In addition, synchronized locomotor force and kinematic data allow analyses of joint equilibrium that document external and muscular forces and moments acting on limb bones. Although these analyses produce indirect estimates of load magnitudes, they provide insight into the mechanics underlying bone loading patterns (i.e. how forces are transmitted to bones) that direct *in vivo* strain measurements cannot supply (Biewener and Full, 1992). Therefore, in the context of our complementary study of limb bone strains in these species (Blob and Biewener, 1999), this study helps to clarify the mechanical differences between non-parasagittal and parasagittal locomotion and, thereby, evaluates the functional changes entailed in evolutionary transitions from sprawling to non-sprawling posture.

Materials and methods

Experimental animals

Data were collected from four subadult green iguanas *Iguana iguana* (Linnaeus) (body mass 320–516 g) and one juvenile American alligator *Alligator mississippiensis* (Daudin) (body mass 1.98 kg) that also were used in experiments to measure *in vivo* limb bone strain (Blob and Biewener, 1999). Animal care and housing are described in the strain study. All experimental procedures followed University of Chicago IACUC guidelines (protocols 61341 and 61371). After bone strain recordings had been completed, the animals were killed (Nembutal sodium pentobarbital, 200 mg kg^{-1} intraperitoneal injection) and frozen for later dissection and measurement of anatomical variables.

Collection of kinematic and force data

Animals were filmed using high-speed video (Kodak EktaPro, model 1012 image-intensified system) while running over a custom-built force platform inserted into a 6 m long wooden trackway (Biewener and Full, 1992). Video framing rate was 500 frames s^{-1} for *I. iguana* and 250 frames s^{-1} for *A. mississippiensis*. Between 18 and 34 frames (evenly spaced in time) were digitized for each step, depending on step duration (steps are defined as the period of foot contact with the ground). This produced effective framing rates of 71–167 frames s^{-1} for *I. iguana* and 25–50 frames s^{-1} for *A. mississippiensis*. To facilitate digitization of joint positions, dots of white latex were painted on the claw of the fourth digit, the metatarso-phalangeal joint, the ankle, knee and hip joints and the posterior ilium. Room temperature was 25 °C, but before and after trials animals were allowed to rest and bask under heat lamps, where the temperature was the same as in the enclosure in which they were housed (29–32 °C).

The surface of the force platform was flush with that of the track, and both were covered with thin rubber to give the animals sufficient friction to prevent slipping. A 1.1 m Plexiglas panel lateral to the force platform allowed the right side of the animal to be videotaped as it ran past the camera and over the platform. Dorsal and lateral views were filmed simultaneously using a mirror positioned over the force platform at 45 ° to the track surface. Joint positions were digitized from video frames in both views (Measurement TV; Updegraff, 1990). These two sets of coordinate data were used to calculate limb kinematics in three dimensions in a custom-designed Pascal program. Prior to kinematic calculations, coordinate data were filtered digitally with a zero-lag, second-order, low-pass Butterworth filter (cut-off frequency 4–6 times stride frequency) and corrected for parallax. The cut-off frequencies employed removed noise without attenuating signal peaks. Unless stated otherwise, reported angles are true angles (in three dimensions) between segments.

Force platform design was adapted from that outlined by Biewener and Full (Biewener and Full, 1992) and allowed the vertical, anteroposterior and mediolateral components of the ground reaction force to be resolved. A rectangular (20 cm×25 cm) panel of honeycomb aluminum was bonded to four brass beams and supported over a metal base. Three single spring blades were machined from each support (one for each direction of force measurement), and single-element metal foil strain gauges (Tokyo Sokki Kenkyujo Co., type FLA-1-11) were bonded to both sides of each blade. Circuits were configured to allow separate recording of forces from each of the four vertical blades (which were then summed to calculate total vertical force) and single force outputs in the anteroposterior and mediolateral directions. Raw force signals from the six channels were output to Vishay conditioning bridge amplifiers (model 2120; Measurements Group),

sampled through an A/D converter at 500 Hz and stored on computer. The plate was designed to accommodate a 50 N vertical load; amplifier gains for each channel were adjusted appropriately for the weight of the animal to allow more sensitive resolution of forces. Calibrations verified that the response of the platform to loads was linear over the range of forces recorded. The natural unloaded frequencies of the platform were 210 Hz (vertical), 150 Hz (anteroposterior) and 75 Hz (mediolateral), all sufficiently greater than the stride frequencies of the animals studied (less than 4 Hz in both species) so as not to confound the signal produced by the ground reaction force. Cross-talk between channels (<3 %) was corrected in the data-analysis software. Force data were filtered digitally with a zero-lag, second-order, low-pass Butterworth filter (cut-off frequency ⩾10.5 times stride frequency) prior to analysis. The point of application of the ground reaction force was calculated initially as half the distance between the toe and ankle. As the heel lifted off the substratum, the point of application was recalculated for each frame as half the distance between the toe and the most posterior part of the foot contacting the ground. Thus, the ground reaction force shifted anteriorly through the step so that it was applied at the end of the toes by the end of the support phase (Carrier et al., 1994).

Steps in which the right hindfoot contacted the force platform in isolation were selected for analysis. However, the behavior of the animals was difficult to control, and such steps were uncommon for the alligator. Therefore, additional steps were analyzed in which the right hindfoot was in isolated contact with the platform prior to peak force (i.e. overlapping contact by the right forefoot did not influence measurements of peak forces). All steps with left limb contact or substantial tail contact with the plate were excluded. The Pascal program used for kinematic analysis also synchronized force and kinematic data, with the beginning of the force traces indicating the beginning of foot contact with the platform (i.e. the first video frame digitized). Calculations of force components in particular directions and joint moments due to the ground reaction force then were performed. Inertial and gravitational moments about the hindlimb joints were assumed to be negligible during stance because they are typically small relative to the moments produced by the ground reaction force during stance (Alexander, 1974; Biewener and Full, 1992).

Anatomical definitions

To facilitate calculations of locomotor stresses in the limb bones of *A. mississippiensis* and *I. iguana*, forces acting on their limbs were resolved into a frame of reference defined by the anatomical planes of the limb segments (Fig. 1). To distinguish between this anatomical frame of reference and the absolute frame of reference, descriptions of anatomical surfaces and directions of forces and moments in the anatomical frame of reference are placed in quotation marks. The anatomical 'anteroposterior' plane was defined as the plane including the long axes of the tibia and femur. The anatomical 'dorsoventral' plane then was defined as the plane including the long axis of the femur that is perpendicular to the 'anteroposterior' plane, and the anatomical 'mediolateral' plane was defined as the plane including the long axis of the tibia that is perpendicular to the 'anteroposterior' plane (Fig. 1A). Thus, the fibula is 'posterior' to the tibia in the anatomical frame of reference and the knee and ankle flex and extend within the anatomical 'anteroposterior' plane. Following these definitions, the direction of a motion or force is not the same as the plane in which the motion or force occurs. For instance, a dorsally directed force (tending to abduct the femur) will lie within the anteroposterior plane; similarly, during knee flexion, the tibia moves in a 'medial' direction, but within the 'anteroposterior' plane (i.e. the plane with anterior and posterior surfaces).

The anatomical planes change orientation (relative to the absolute frame of reference) through the step. For instance, axial rotation and retraction of the femur cause the anatomical 'dorsoventral' plane to rotate anteriorly and laterally in an absolute frame of reference; with sufficient rotation through stance, the anatomical 'dorsal' surface comes to face anteriorly and the 'anterior' surface to face ventrally (Fig. 1B). Consequently, moments at the joints and forces on the limb change in the anatomical frame of reference, even if the orientation of the ground reaction force remains constant. If the ground reaction force were oriented vertically throughout the step, it would exert a 'dorsally' directed force and an 'abductor' moment at the hip when the femur is in the position illustrated in Fig. 1A, but a 'posterior' force and 'retractor' moment at the hip when the femur is in the position illustrated in Fig. 1B.

Bone stress analyses

Both the ground reaction force and the forces exerted by limb muscles induce stress in the limb bones during locomotion. Stresses in the femur and tibia were calculated at midshaft, where empirical studies have shown that bending moments are typically greatest (e.g. Biewener and Taylor, 1986). To evaluate forces and moments acting at midshaft, the limb bones were modeled as beams; forces and moments acting at midshaft can be determined by 'cutting' each beam at that point and constructing a free body diagram of either half (Beer and Johnston, 1997). We constructed free body diagrams for the distal half of each bone (Alexander, 1974; Biewener et al., 1983). Therefore, only forces acting on the distal half of each bone, including the ground reaction force and forces exerted by muscles inserting distal to midshaft, entered directly into our calculations of peak bending stress. For the purposes of this analysis, limb muscle arrangements are essentially similar in *I. iguana* and *A. mississippiensis* (Fig. 2; Table 1). Anatomical differences between lizards and crocodilians (e.g. the lack of a calcaneal tuber and the presence of a pubotibialis muscle in lizards) affect specific calculations, but do not affect the underlying analyses of muscle forces and bone stresses.

To calculate muscle forces, the limb joints were assumed to be in static rotational equilibrium (Alexander, 1974; Biewener, 1983a; Biewener and Full, 1992). A further initial assumption was made that the only muscles active at a joint were those

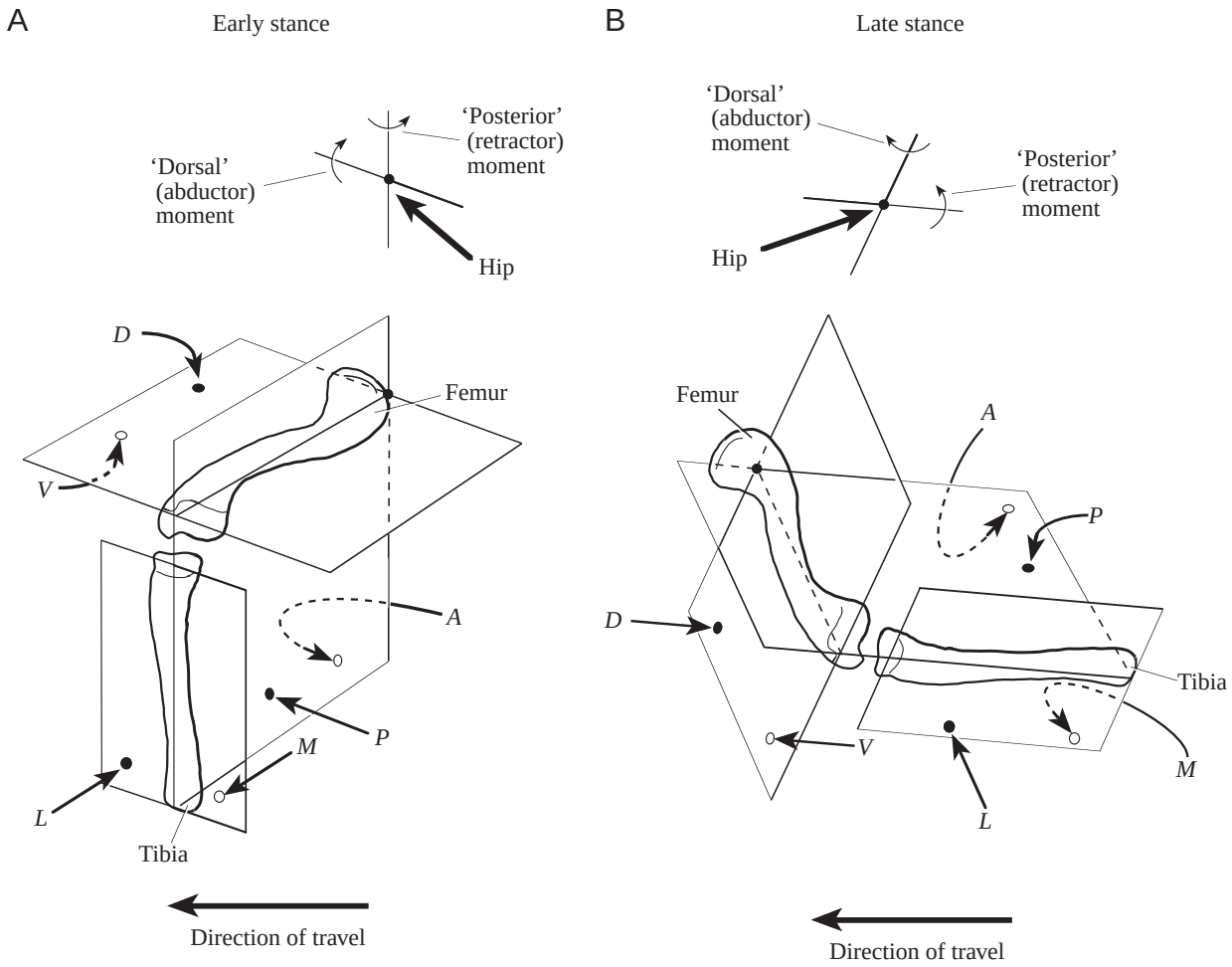

Fig. 1. Outline sketches (left lateral view) of the femur and tibia of *Alligator mississippiensis* illustrating the planes defining the anatomical frame of reference for force platform analyses and changes in the orientation of those planes from early stance (A) to late stance (B). The fibula is omitted for clarity. Both surfaces of each plane are labeled, with solid arrows and filled circles indicating surfaces in view and dashed arrows and open circles indicating surfaces hidden from view (i.e. surfaces that only can be seen if the planes are transparent). *A*, anterior; *D*, dorsal; *L*, lateral; *M*, medial; *P*, posterior; *V*, ventral. Above each sketch of the skeletal elements, moments at the hip joint are illustrated and defined in the anatomical frame of reference.

acting to counter the rotational moment caused by the ground reaction force (i.e. antagonist muscles that would augment moments due to the ground reaction force were assumed to be inactive). Under these assumptions, the muscle forces (F_m) necessary to maintain equilibrium at a joint can be calculated as:

$$F_m = (M_{GRF}/r_m), \quad (1)$$

where M_{GRF} is the moment of the ground reaction force at the joint and r_m is the moment arm of the muscles countering the moment of the ground reaction force (Alexander, 1974; Biewener, 1983a; Biewener, 1989). Where multiple muscles contributed to resisting rotation at a joint, a weighted mean moment arm was calculated for the muscle group on the basis of the cross-sectional areas of each muscle, which are assumed to be proportional to the contributions of each muscle to the total force the group exerts (Alexander, 1974; Biewener and Full, 1992). Muscle cross-sectional areas were calculated as described previously (Biewener and Full, 1992).

Limb muscles placing stress on the femur and tibia span the ankle, knee and hip joints. Because the ground reaction force generates a flexor moment at the ankle for nearly all of stance (see Results), only extensor muscles must be considered at the ankle, and calculation of the force they exert is straightforward. On the basis of anatomical relationships, Schaeffer (Schaeffer, 1941a) and Snyder (Snyder, 1954) proposed that the gastrocnemius, flexor digitorum longus and peroneus longus extend the ankle in lizards and crocodilians. Electromyographic (EMG) data from *Sceloporus clarkii* (Reilly, 1994/95; Reilly, 1998) support this interpretation for the gastrocnemius and peroneus longus in iguanian lizards, and EMG data from *Caiman crocodilus* (Gatesy, 1997) support this interpretation for the gastrocnemius in crocodilians. All three muscles were considered to be ankle extensors in the present study.

Evaluation of muscle forces acting on the femur is complicated by the multiple muscle groups crossing the hip and knee joints (Fig. 2). The model of muscle forces applied

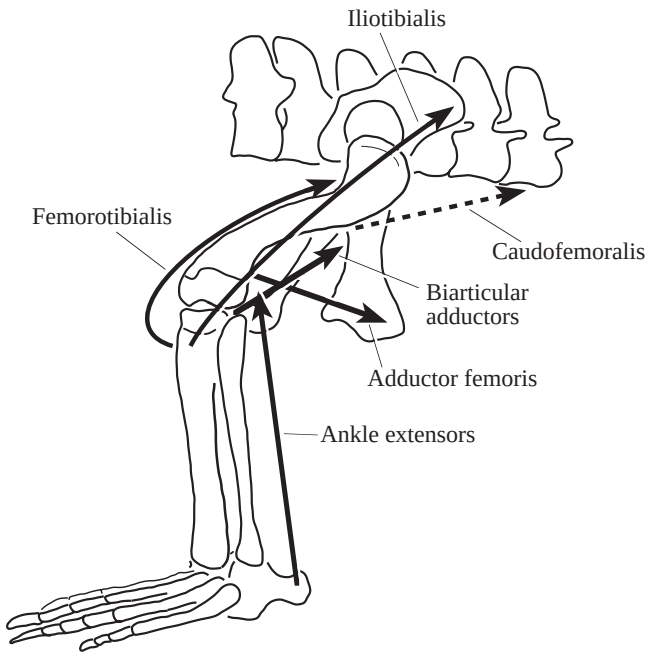

Fig. 2. Outline sketch (left lateral view) of the hindlimb skeleton of *Alligator mississippiensis* illustrating the lines of action of the major muscle groups contributing to stress in the femur and tibia during stance. Muscle forces could not be calculated for the caudofemoralis (dashed arrow; see text).

to the femur is described fully in the Appendix; the primary features are as follows. (i) Muscle groups are assumed to act in the same anatomical plane throughout stance. (ii) The caudofemoralis is the only muscle active during stance in the 'anteroposterior' direction; however, its main insertion is proximal to midshaft. Thus, 'anteroposterior' midshaft bending calculations are derived exclusively from the ground reaction force, using a free body diagram of the distal half of the femur. (iii) Hip adductors (the adductor femoris, puboischiotibialis, flexor tibialis internus, pubotibialis in lizards only) counter the 'abductor' ('dorsally' directed) moment of the ground reaction force at the hip early in stance and bend the femur to place its 'ventral' cortex in compression. Adductors spanning the knee joint also augment the knee flexor moment of the ground reaction force, but adductor activity ceases late in stance when rotation of the femur causes the moment of the ground reaction force to change direction (i.e. to become an 'adductor' moment). (iv) Knee extensors (the femorotibialis and iliotibialis) on the 'dorsal' surface of the femur counter the combined knee flexor moments of the ground reaction force and the hip adductors and ankle extensors that span the knee. The bending moment induced by knee extensors on the femur opposes that induced by hip adductors, placing the 'dorsal' cortex of the femur in compression. In addition, the iliotibialis (which spans the hip) is assumed to counter the ground reaction force moment at the hip when it becomes an 'adductor' moment late in stance. Because the actions of muscles crossing both the hip and knee oppose each other, there is no unique solution to muscle force calculations; however, the model applied in this study accounts for known co-activation of antagonist muscle groups to the extent that is possible. Muscle force calculations were made for every digitized frame of each step using a custom-designed Matlab (MathWorks) program.

Table 1. *Mean anatomical data from hindlimb muscles of experimental animals*

	Iguana iguana (*N*=4)			*Alligator mississippiensis* (*N*=1)		
Muscle	*A*	θ	r_m	*A*	θ	r_m
Hip adductors						
Adductor femoris	24.0	9	10.1^{h}	28.8	17	19.3^{h}
Puboischiotibialis	29.9	13	14.5^{h}, 3.7^{k}	9.6	17	19.3^{h}, 9.1^{k}
Pubotibialis	15.2	9	10.1^{h}, 3.3^{k}	–	–	–
FTI 1 (I)	13.3	13	14.5^{h}, 4.5^{k}	36.4	17	19.3^{h}, 12.9^{k}
FTI 2s (II)	19.6	13	14.5^{h}, 2.6^{k}	22.7	17	19.3^{h}, 12.9^{k}
FTI 2d (III)	9.5	9	10.2^{h}, 3.4^{k}	16.5	12	19.3^{h}, 9.5^{k}
Knee extensors						
Femorotibialis	93.5	0	5.0^{k}	185.3	0	8.2^{k}
Iliotibialis	33.1	15	13.8^{h}, 5.0^{k}	80.9	15	15.5^{h}, 8.2^{k}
Ankle extensors						
Gastrocnemius	129.6	0	4.2^{a}, 2.3^{k}	109.9	0	10.7^{a}, 6.8^{k}
Peroneus longus	25.2	0	2.6^{a}, 1.6^{k}	34.9	0	6.0^{a}, 4.5^{k}
FDL (I+II)	35.9	0	3.1^{a}, 1.6^{k}	59.8	0	6.9^{a}, 4.5^{k}

A, cross-sectional area of muscle (in mm^2); θ, angle between the muscle and the long axis of the bone (in degrees); r_m, moment arm of the muscle (in mm) about the joint indicated by the superscript letter (h, hip; k, knee; a, ankle); FDL, flexor digitorum longus; FTI, flexor tibialis internus.

By convention, individual muscles in the FTI complex are identified by arabic numerals for *Iguana iguana* (s and d refer to superficial and deep muscles) and roman numerals for *Alligator mississippiensis*.

The pubotibialis is absent from *Alligator mississippiensis*.

Muscular contributions to limb bone torsion were not estimated. The tibial insertions of muscle groups active during stance are primarily in the plane of knee flexion and extension and are unlikely to promote substantial torsion; therefore, tibial torsion was assumed to be caused by the ground reaction force alone. However, the primary stance phase retractor of the femur in lizards and crocodilians, the caudofemoralis, inserts 'ventrally' on the femur and, thus, causes rotation of the femur about its long axis during retraction (Snyder, 1962; Gatesy, 1997). For most of stance, the caudofemoralis acts to produce moments at the hip that augment those due to the ground reaction force, both as a retractor and as a femoral rotator (see Results); therefore, calculations of caudofemoralis force based on joint equilibrium cannot be made without further assumptions about the activity of its antagonists. Rather than make such assumptions, torsional moments for the femur were calculated as though they had been induced by the ground reaction force alone. Torsional moments and stresses are almost certainly higher than indicated by these minimum estimates.

After calculation of muscle forces, the bending moments and axial and bending stresses acting in the limb bones were evaluated following published methods (Biewener, 1983a; Biewener and Full, 1992), with modifications for three-dimensional stress analysis. Anatomical data for skeletal elements from experimental animals are reported in Table 2. Compressive axial stresses (σ_{ax}) in the midshafts of the femur and tibia were calculated as:

$$\sigma_{ax} = -[\sum(F_m\cos\theta_{ax}) + GRF_{ax}]/A\,, \quad (2)$$

where θ_{ax} is the weighted mean angle between each muscle group and the long axis of the bone, $\sum(F_m\cos\theta_{ax})$ is the sum of muscle force components acting along the bone axis, GRF_{ax} is the component of the ground reaction force acting along the bone axis and A is the cross-sectional area of the bone at midshaft. To calculate the cross-sectional area of each element, the limb bones excised from the killed animals were cut at midshaft, and a magnified tracing of each cross section was made. Endosteal and periosteal outlines from these tracings were entered into a computer using a digitizing tablet, and area calculations were made using a custom-designed QuickBasic routine.

To calculate bending stresses acting at the midshafts of the bones, bending moments induced by transverse components of the ground reaction force (GRF_{tr}) and axial components of the ground reaction force acting about the longitudinal curvature of the bone (GRF_{ax}), together with the net bending moment induced by muscular forces (F_m), were calculated for each bone in each of the two perpendicular planes illustrated in Fig. 1. Forces and moments considered in these calculations are illustrated in the 'dorsoventral' direction for the femur in Fig. 3. The moment due to the transverse component of the ground reaction force at midshaft (M_{tr}) was calculated as:

$$M_{tr} = GRF_{tr}(L/2)\,, \quad (3)$$

where L is the length of the bone. The bending moment induced by the axial component of the ground reaction force due to bone curvature (M_c) was calculated as:

$$M_c = GRF_{ax}r_c\,, \quad (4)$$

where r_c is the moment arm of GRF_{ax} due to bone curvature (Biewener, 1983a; Biewener, 1983b). Values of r_c were measured from outline sketches of the bones traced from photographs of each specimen in the defined anatomical views. Because the limb muscles insert on the bone cortices, muscular forces act at a distance from the central axis of the bone. Therefore, the midshaft bending moment induced by each muscle group (M_m) was calculated as the vector cross product of the muscle force (F_m) and the moment arm of the muscles about the midshaft centroid (Beer and Johnston, 1997):

$$M_m = F_m(r_b\sin\theta_b)\,, \quad (5)$$

where r_b is the distance between the centroid and the point of application of muscle force on the bone surface, and θ_b is the angle between r_b and the line of action of the muscle.

After calculating the net bending moment acting in each of the perpendicular anatomical directions for each bone ($M_{b/dir}$), the bending stress in each direction ($\sigma_{b/dir}$) was calculated as:

$$\sigma_{b/dir} = M_{b/dir}(y/I)\,, \quad (6)$$

where y is the distance from the neutral axis of bending to the bone cortex in the direction under consideration, and I is the second moment of area for bending about that neutral axis.

Table 2. *Mean anatomical data from hindlimb bones of experimental animals*

	Iguana iguana (N=4)		*Alligator mississippiensis* (N=1)	
	Femur	Tibia	Femur	Tibia
Length (mm)	55.1	42.2	61.5	50.7
A (mm^2)	6.22	4.53	18.30	11.90
$r_{c(x)}$ (mm)	–0.22	1.23	–0.05	0.26
$r_{c(y)}$ (mm)	1.75	–1.71	1.36	–1.65
y_x (mm)	2.0	1.7	3.0	2.1
y_y (mm)	2.2	1.7	3.3	2.1
I_x (mm^4)	9.34	5.27	57.00	15.48
I_y (mm^4)	10.69	4.86	67.13	16.16
J (mm^4)	20.03	10.13	124.13	31.64

Subscript x denotes the anatomical 'anteroposterior' direction for the femur and tibia; subscript y denotes the 'dorsoventral' direction for the femur or the 'mediolateral' (flexion–extension) direction for the tibia (see Fig. 1 for definitions).

A, cross-sectional area of bone; r_c, moment arm due to bone curvature; y, distance from neutral axis to bone cortex; I, second moment of area; J, polar moment of area.

Data from the tibia are not corrected for the effects of the fibula.

Curvature sign conventions: femur$_x$, + = concave 'posterior', – = concave 'anterior'; femur$_y$, + = concave 'ventral', – = concave 'dorsal'; tibia$_x$, + = concave 'posterior', – = concave 'anterior'; tibia$_y$, + = concave 'lateral', – = concave 'medial'.

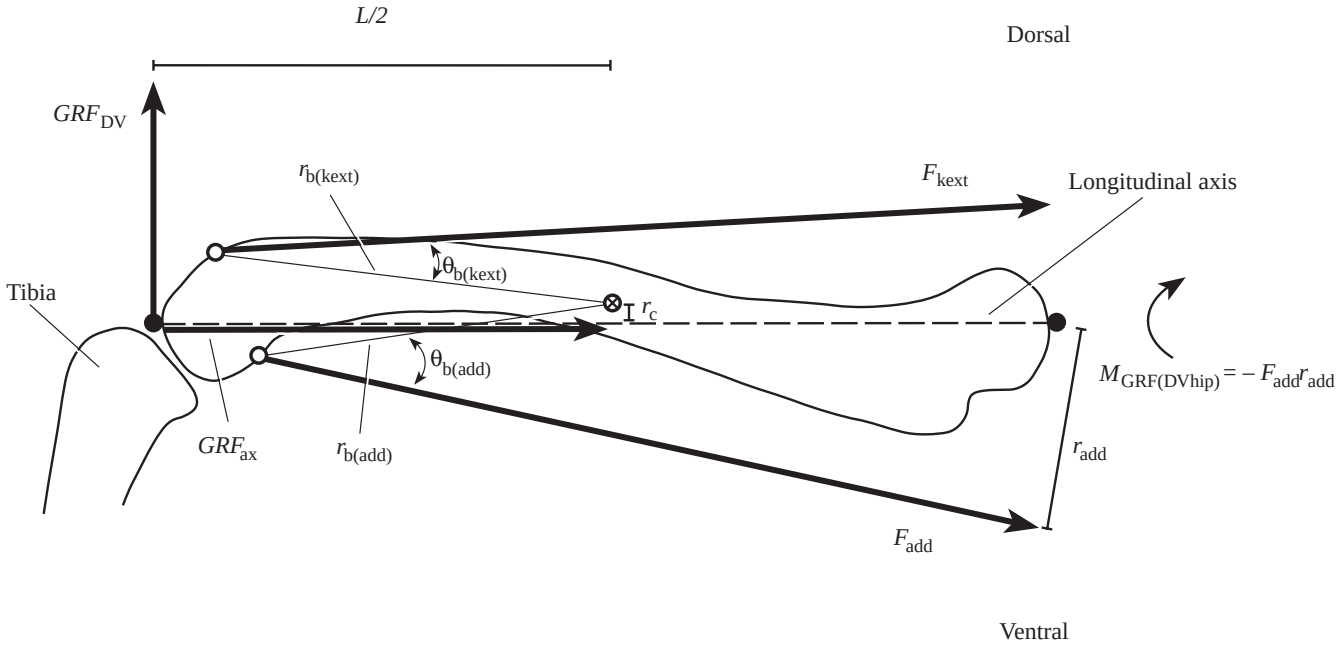

Fig. 3. Anterior view diagram of the femur and proximal tibia of *Iguana iguana* illustrating the forces and moments acting in the anatomical 'dorsoventral' direction. The centers of the proximal and distal articular surfaces are indicated by filled circles; points of application of adductor and knee extensor muscles (i.e. proximal extents of distal articular surface) are indicated by open circles; ⊗ indicates the midshaft centroid of the femur. GRF_{ax}, the component of the ground reaction force acting along the long axis of the femur; r_c, the bending moment arm of GRF_{ax} due to bone curvature; GRF_{DV}, the component of the ground reaction force acting transverse to the femur in the 'dorsoventral' direction; $L/2$, the bending moment arm of GRF_{DV} about the midshaft of the femur (half femur length); $M_{GRF(DVhip)}$, the moment of the ground reaction force about the hip; F_{kext}, the force exerted by the knee extensor muscles; $r_{b(kext)}$, the moment arm of the knee extensors about the midshaft centroid; $\theta_{b(kext)}$, the angle between $r_{b(kext)}$ and the line of action of the knee extensors; F_{add}, the force exerted by the hip adductor muscles; r_{add}, the moment arm of the hip adductors about the hip; $r_{b(add)}$, the moment arm of the hip adductors about the midshaft centroid; $\theta_{b(add)}$, the angle between $r_{b(add)}$ and the line of action of the hip adductors. Net lines of action of the knee extensors and hip adductors are illustrated. Force vectors are not drawn to scale.

Both y and I were calculated from the digitized limb bone sections used to calculate cross-sectional area (Table 2). The magnitude of net bending stress ($\sigma_{b/net}$) in the midshaft section was calculated as the vector sum of the stresses in the two perpendicular anatomical planes for each bone. In the femur, for instance:

$$\sigma_{b/net} = (\sigma_{b/DV}^2 + \sigma_{b/AP}^2)^{0.5}, \quad (7)$$

where DV and AP refer to the 'dorsoventral' and 'anteroposterior' directions, respectively. The orientation of peak bending stress was also calculated. For the femur, the angular deviation of peak stress from the 'anteroposterior' axis ($\alpha_{b/net}$) is:

$$\alpha_{b/net} = \tan^{-1}(\sigma_{b/DV}/\sigma_{b/AP}). \quad (8)$$

The net neutral axis of bending is perpendicular to this axis. Net longitudinal stresses at the points of peak tensile and compressive bending stress then were calculated as the sum of axial and bending stresses. Torsional stress (τ) due to the ground reaction force was also calculated:

$$\tau = T(y_t/J), \quad (9)$$

where T is the torsional moment applied to the bone by the ground reaction force, y_t is the distance from the centroid of the bone to its cortex and J is the polar moment of area (Wainwright et al., 1976). J was calculated from each digitized cross section, and y_t for each section was calculated as the average of the y values for the two perpendicular anatomical directions (Table 2).

In stress calculations for the tibia, additional steps were required to account for contributions of the fibula to load-bearing in the crus. In both *I. iguana* and *A. mississippiensis*, the fibula is robust, and the distance between the tibia and fibula is large; therefore, failure to consider the fibula could lead to substantial overestimation of tibial stresses. To evaluate the effects of the fibula on tibial stresses, calculations of y and I in the 'anteroposterior' and 'mediolateral' anatomical directions, and of y_t and J, were made from a cross section of an articulated tibia and fibula from an iguana similar in size to the experimental animals used in this study (Fig. 4). The ratio y_t/J and the ratios y/I for each of the two anatomical planes then were calculated to determine scaling factors to apply to the initial tibial stress calculations. The relative cross-sectional areas of the tibia and fibula also were calculated to assess the contribution of the fibula to resistance to axial stresses. These calculations indicated that, to account for stress resistance imparted by the fibula, tibial stresses should be multiplied by the following correction factors: 'anteroposterior' stress, 0.11; 'mediolateral' stress, 0.53; shear stress, 0.37; axial

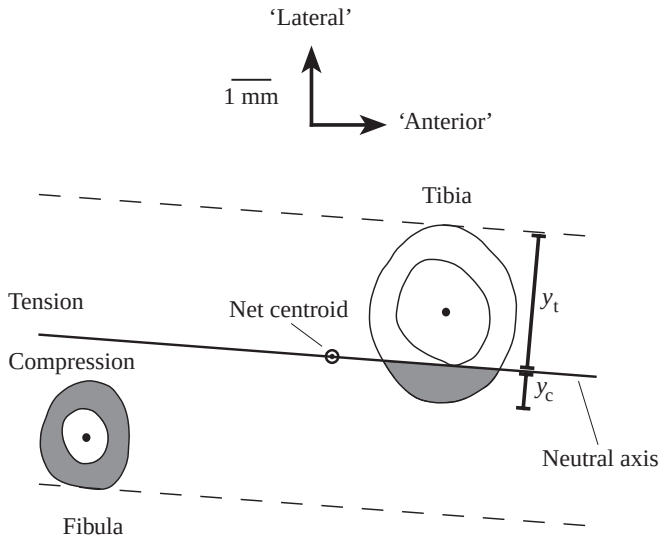

Fig. 4. Midshaft cross sections of the tibia and fibula of *Iguana iguana* illustrating their relative positions in the crus and the displacement of the neutral axis of bending away from the centroid of either bone (filled circles) to the net centroid of the section. Rotation of the neutral axis is based on the results of the experiments. Portions of the bones experiencing compression are shaded; portions experiencing tension are unshaded. Because of the displacement of the neutral axis to the net centroid, the distance from the neutral axis to the 'medial' cortex of the tibia (y_c) is smaller than the distance from the neutral axis to the 'lateral' cortex (y_t), placing the tibia in net tension and the fibula in compression.

compressive stress, 0.67. The effect of the fibula is to shift the net centroid of the combined section of the tibia and fibula 'posteriorly' and 'medially'. Consequently, the 'posterior' and 'medial' cortices of the tibia contribute less to stress resistance than the 'lateral' and 'anterior' cortices. The effect of this shift in the neutral axis on values of y was taken into account and applied to calculations of stress for those surfaces (Fig. 4). These corrections were based on *I. iguana*, so they are a potential source of error for calculations of stress in the *A. mississippiensis* tibia. In addition, calculations of y, I, y_t and J from the combined tibial and fibular sections assume that no motion is possible between the tibia and fibula (i.e. that shear is transferred completely across both elements). Although some motion of the tibia relative to the fibula appears to occur in lizards and crocodilians (Rewcastle, 1980; Landsmeer, 1990; see also tracings from X-ray cine frames in Brinkman, 1980a; Gatesy, 1991), this motion is highly restricted. Therefore, it seems likely that conservative calculations accounting for fibular load bearing will be better estimates of actual stresses in the tibia than values that do not.

Calculation of limb bone safety factors

Safety factors were calculated for the femur and tibia in *I. iguana* and *A. mississippiensis* as the ratio of tensile yield stress to peak tensile locomotor stress. 'Mean' safety factors were calculated from the mean values of peak stress and mechanical properties. In addition, when error ranges for peak stress and mechanical property values were available, 'worst-case' (i.e. lowest possible) safety factors were calculated on the basis of mean yield stress minus 2 S.D. and mean peak stress plus 2 S.D.

Peterson and Zernicke (Peterson and Zernicke, 1987) report a value of 218 MPa (no error range) for the tensile yield stress of the tibia of *Dipsosaurus dorsalis*, an iguanian lizard closely related to *I. iguana* (Norell and de Queiroz, 1991; Petren and Case, 1997). We used this value to calculate safety factors for the femur and tibia of *I. iguana*. Currey (1988) reported a value of 12.0±2.4 GPa (mean ± S.D., N=6) for the stiffness of *A. mississippiensis* femur in bending. Estimates of tensile yield stress in bending were calculated by multiplying Currey's (Currey, 1988) stiffness value by 6495 με (tensile yield strain for alligator femur; Blob and Biewener, 1999), producing a mean yield stress of 78.1 MPa and a 'worst-case' yield stress of 46.6 MPa. These yield stress estimates for *A. mississippiensis* appear low, but are reasonable when compared with Currey's (Currey, 1990) published value for the ultimate stress of alligator femur (108 MPa) and are derived in part from independently collected data (Blob and Biewener, 1999).

Tests of correlations between limb bone stress and limb posture

Because of the small sample size of steps obtained from *A. mississippiensis*, correlations between limb bone stress and limb posture were tested only in *I. iguana*. Measurements of the angle of the femur below the horizontal at the time of peak stress were extracted from the kinematic calculations for each run. Peak tensile and compressive stresses in the femur, together with stresses calculated for the anterior and dorsal cortices, were then regressed (least-squares) on these posture angles to evaluate the relationship between limb posture and load magnitude and to assess the degree of correspondence with patterns observed during strain measurements. Reduced major axis (RMA) slopes were calculated for regressions with significant correlation coefficients. RMA is the most appropriate method of regression for the evaluation of structural relationships between variables when both are subject to error (McArdle, 1988; LaBarbera, 1989).

Analyses of bone strain in alligators (Blob and Biewener, 1999) suggested that tensile strains on the 'anterior' cortex of the femur decrease with more upright posture, but tensile strains on the 'ventral' cortex and compressive strains on the 'dorsal' cortex increase with more upright posture. 'Anterior' tensile strains (or stresses) could decrease if axial compression increased as posture became more upright. However, increases in 'dorsal' and 'ventral' femoral stresses (and strains) could result from one of two alternative mechanisms. (i) Hip adductor muscles (on the 'ventral' femur) bend the femur in the opposite direction from the ground reaction force; thus, if adductors exert less force during more upright steps, they would mitigate bending due to the ground reaction force less effectively, causing higher 'dorsal' and 'ventral' stresses. Reduced adductor force could result from decreases in the hip abductor moment of the ground reaction force during more

upright posture, which would occur if the ground reaction force either acts closer to the hip or decreases in magnitude during more upright steps. (ii) Alternatively, an increase in the force exerted by the knee extensor muscles (on the 'dorsal' femur) with upright stance, rather than a decrease in hip adductor force, might cause higher dorsoventral stresses. Increased knee extensor force could result from increases in the flexor moment at the knee, which would occur if ground reaction force magnitude, its moment arm at the knee, or the forces exerted by the knee flexor muscles (e.g. biarticular ankle extensors) were greater in more upright steps. To differentiate between these mechanisms, we regressed the following variables (for each filmed step) on femoral posture: the moment arms of the ground reaction force at the hip, knee and ankle at peak stress; the magnitude of the ground reaction force; and the magnitudes of the forces exerted by each major muscle group.

Statistical notes

Differences between group means were tested using non-parametric Mann–Whitney *U*-tests unless noted otherwise. Error ranges reported for all measurements are one standard deviation (S.D.).

Results

Overview of loading mechanics for the femur and tibia of I. iguana *and* A. mississippiensis

The mechanics of skeletal loading in *I. iguana* and *A. mississippiensis* hindlimbs are sufficiently similar to be summarized together as follows. Detailed results are provided in the sections that follow.

At the beginning of stance, the tibia is oriented nearly vertically and the femur is directed with its distal end anterior and ventral to its proximal end (Fig. 5). The ground reaction force is directed posteriorly and medially, exerting flexor moments at the ankle and knee and 'dorsal' ('abductor') and 'posterior' moments at the hip (Figs 6, 7). The ground reaction force also exerts torsional moments tending to rotate the right femur counterclockwise about its long axis if viewed from its proximal end and the right tibia clockwise if viewed from its proximal end (Fig. 7). Ground reaction force moments are countered by ankle extensors at the ankle and by hip adductors at the hip. Both of these add to the flexor moment produced at the knee by the ground reaction force, which is countered by the knee extensors. These muscular forces add to the axial components of the ground reaction force, compressing both elements and, with transverse components of the ground reaction force, applying bending moments about the midshaft of each bone. The bending moment induced on the tibia by the ground reaction force is in the plane of flexion and extension, summing with the bending moment of the ankle extensors to place the 'lateral' (dorsiflexor) surface in tension and the 'medial' (plantarflexor) surface in compression (Figs 8, 9). Through the beginning of stance, the hip adductors exert a moment that bends the femur 'ventrally', but the summed moment of the knee extensors and ground reaction force is larger and opposes the adductors, producing a net moment tending to bend the femur 'dorsally' (i.e. placing its 'dorsal' surface in compression; Figs 8, 9). In the 'anteroposterior' direction, the bending moment induced by the ground reaction force places the 'posterior' cortex of the femur in compression; thus, the femur bends about an 'anterodorsal–posteroventral' axis to place its 'posterodorsal' cortex in compression and its 'anteroventral' cortex in tension. In addition to bending, both bones experience torsion and axial compression.

Through stance, ground reaction force magnitude increases and its orientation shifts anteriorly, but its medial inclination is slight (Fig. 6). By the time of peak stress (approximately mid-stance), the proximal end of the tibia rotates anteriorly and laterally relative to its distal end and the heel lifts off the ground, raising the distal tibia with respect to the proximal tibia (Fig. 6). Bending moments acting on the tibia become large in the 'mediolateral' (flexor–extensor) direction as the tibia is oriented nearly perpendicular to the ground reaction force and the ankle extensors must exert larger forces to counter increases in the ankle flexor moment (Figs 6–8). The femur adducts slightly, retracts to nearly 90 ° to the body, and rotates almost 90 ° about its long axis, shifting its anatomical 'dorsoventral' plane towards the original location of its anatomical 'anteroposterior' plane. With the limb bones in these positions, the ground reaction force maintains a flexor moment at the knee and a torsional moment tending to rotate the tibia 'laterally' (Fig. 7). The 'posterior' bending moment on the femur is maintained as the anatomical 'posterior' direction rotates to face upwards (i.e. dorsal) in an absolute frame of reference, and a larger component of the nearly vertical ground reaction force comes to act in this direction (Fig. 8). However, as the femur rotates axially and retracts, the ground reaction force component in the 'dorsoventral' direction gradually decreases in magnitude, and then increases in the opposite sense from its original direction. Thus, the ground reaction force comes to exert an 'adductor' moment at the hip (although 'adduction' is now aligned close to posterior in an absolute frame of reference) and to bend the femur 'ventrally' (placing the ventral cortex in compression) (Figs 7–9). With these shifts, the bending moment induced by the ground reaction force now opposes that induced by the knee extensors, but the moment of the extensors is larger and maintains the initial orientation of bending (i.e. posterodorsal compression, anteroventral tension). Early in stance, as the hip moves forward over the foot, the line of action of the ground reaction force comes to pass posterior to the long axis of the femur and to exert a torsional moment that augments that of the caudofemoralis (Figs 6, 7).

Kinematics and ground reaction force orientations

Detailed kinematic data were reported for *I. iguana* by Brinkman (Brinkman, 1981) and for *A. mississippiensis* by Gatesy (Gatesy, 1991) and Reilly and Elias (Reilly and Elias, 1998), although at considerably slower speeds (0.35 m s^{-1} for *I. iguana* and 0.15 m s^{-1} for *A. mississippiensis*) than observed in the present study. Kinematic results from the present study

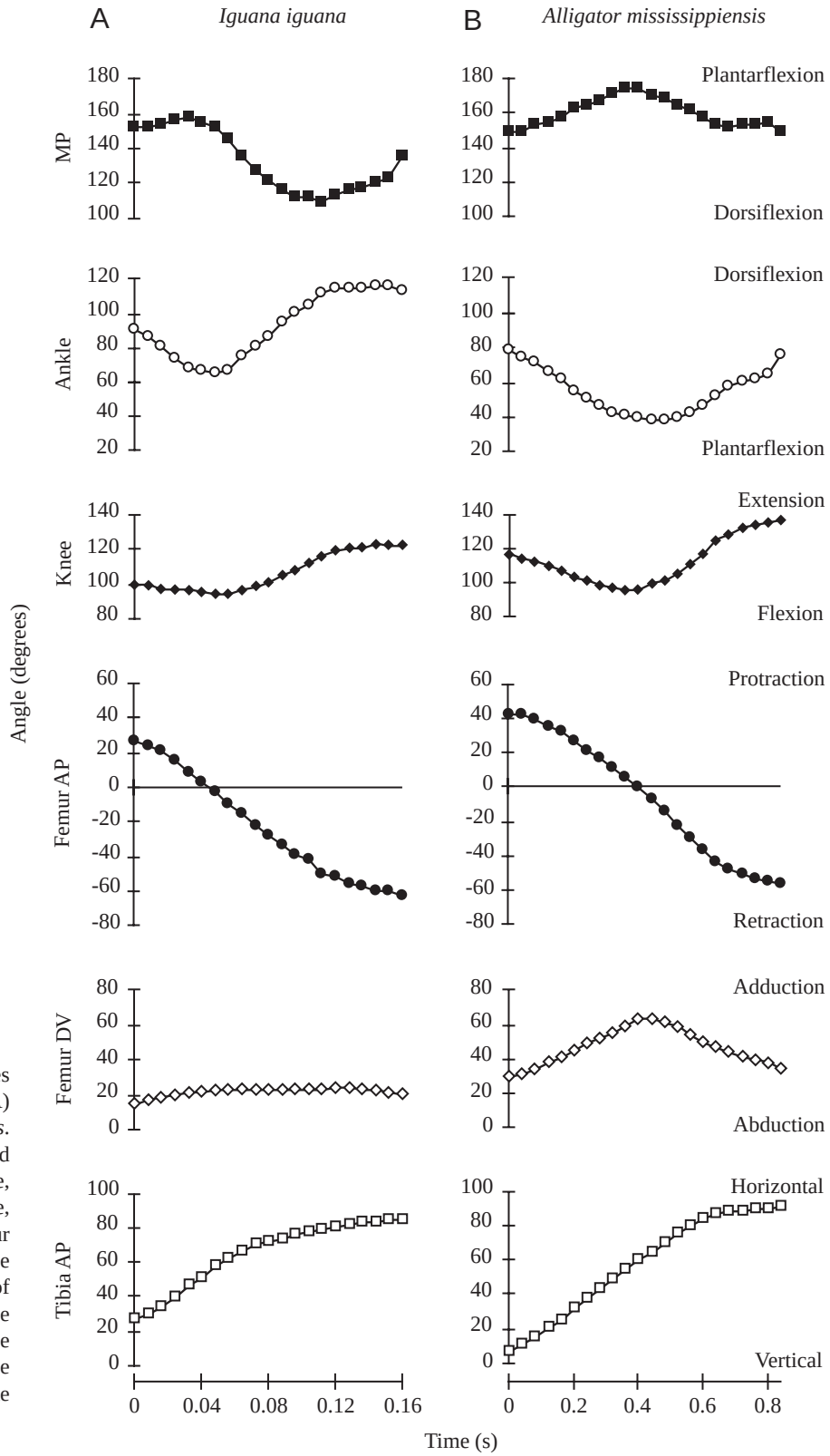

Fig. 5. Kinematic profiles (changes in joint angles over time) for representative steps from (A) *Iguana iguana* and (B) *Alligator mississippiensis*. The symbols on each trace represent the digitized frames. MP, metatarso-phalangeal joint; Ankle, the angle between the tibia and the foot; Knee, the angle between the femur and the tibia; Femur AP, the angle between the femur and the anteroposterior plane (absolute frame of reference); Femur DV, the angle between the femur and the dorsoventral plane (absolute frame of reference); Tibia AP, the angle between the tibia and the anteroposterior plane (absolute frame of reference).

are summarized to provide a context for ground reaction force data and analyses of limb bone loading (Fig. 5). All six trials from the alligator were fast walking trots ($0.62\pm0.21\,m\,s^{-1}$) requiring considerable exertion from the animals (gait designations follow the conventions of Hildebrand, 1976). However, successful trials (isolated right hindfoot falls on the force platform) from iguanas included walking trots ($1.29\pm0.45\,m\,s^{-1}$, N=8), running trots ($1.47\pm0.48\,m\,s^{-1}$, N=8), single-foot diagonal sequence runs ($1.92\pm0.32\,m\,s^{-1}$, N=3) and bipedal running steps ($2.00\pm0.31\,m\,s^{-1}$, N=7). In some cases,

joint angles at which particular movements begin or end (although not necessarily total angular excursions) differ significantly among gaits. However, the timing of particular joint motions (e.g. flexion or extension) generally do not. Furthermore, force measurements and bone stress calculations (see below) do not indicate significant correlations between bone loading and gait or speed over the ranges observed in *I. iguana*. In the context of ground reaction force data, therefore, a single, overall kinematic pattern is described for *I. iguana*. Thus, unless noted otherwise, samples sizes for mean values reported in the following sections are N=6 trials for *A. mississippiensis* and N=26 trials for *I. iguana*.

Kinematics of fast locomotion in I. iguana

The foot is placed flat on the ground at the beginning of stance in *I. iguana*, with the toes angled lateral to the direction of travel. The tibia is usually inclined slightly anteriorly (12±16 °) and medially (8±10 °) from vertical (i.e. the proximal end is anterior and medial to the distal end) (Fig. 5A). The femur is angled anteriorly 43±11 ° from the transverse plane, with the distal end depressed 19±10 ° relative to the proximal end. As Brinkman (Brinkman, 1981) described, initial flexions of the ankle and knee usually precede substantial movement at the hip or metatarso-phalangeal joint. The ankle and knee both form nearly right angles at the start of the step (89±18 ° and 105±19 °, respectively). Both joints are flexed for approximately the first third of the step, reaching angles of 59±15 ° (ankle) and 80±13 ° (knee), after which both joints are extended (to 123±13 ° and 121±14 °, respectively).

During flexion and extension of the knee and ankle, the tibia is inclined further laterally and anteriorly (Figs 5A, 6). Through the first 30–50 % of the step, these movements coincide with retraction and adduction of the femur, with maximum femoral adduction reaching 38±10 ° below horizontal. The femur is abducted as retraction continues after midstep, eventually reaching nearly the same dorsoventral position as at the start of the step (18±6 °). However, by midstep, dorsiflexion at the metatarso-phalangeal joint begins, raising the ankle off the substratum and raising the distal end of the tibia relative to the proximal end. As a result, the tibia continues to be inclined more anteriorly through the step (86±10 °), often placing the ankle higher than the knee late in stance. Lateral inclination of the tibia also increases through midstep, but as the knee is re-extended the tibia becomes more closely aligned with the direction of travel. These rotations of the tibia reflect substantial axial rotation of the femur, such that the anatomical ‘dorsal’ aspect of the femur comes to face anteriorly in an absolute frame of reference. By toe-off, the femur has typically been retracted through an arc of at least 80 °.

Kinematics of fast locomotion in A. mississippiensis

The alligator placed its foot with the toes lateral to the direction of travel (21±5 °), and with a slight upward arch at the metatarso-phalangeal joint (17±5 °) that was flattened through the early portion of the step. The tibia is initially inclined slightly more anteriorly (18±10 °) and less medially (1±6 °) than in *I. iguana* (Fig. 5A,B), although only the difference in medial inclination was significant (P=0.030). The femur is initially 38±8 ° anterior to the transverse plane, similar to *I. iguana*; however, *A. mississippiensis* begins stance with a significantly more adducted femur (34±7 ° below horizontal) than *I. iguana* (P=0.003).

At the beginning of stance, the ankle is slightly more flexed (72±11 °) and the knee slightly more extended (109±11 °) in *A. mississippiensis* than in *I. iguana* (Fig. 5A,B). The ankle is flexed until approximately midstep, closing to 39±4 ° (smaller than *I. iguana*: P<0.001), before extending to nearly 90 °. In contrast to slow walking (Gatesy, 1991), the knee is flexed through the first third of the step during fast locomotion in *A. mississippiensis*. However, knee flexion is approximately 10 ° less than in *I. iguana*, leaving the knee at a significantly greater (P=0.003) obtuse angle (nearly 100 °) when its extension begins.

As in *I. iguana*, the tibia becomes more laterally and anteriorly inclined through the first half of stance in *A. mississippiensis*, coinciding with femoral retraction and adduction (Fig. 5A,B). Femoral adduction reaches a maximum of 68±6 ° below horizontal at midstep, before abducting to return to its starting angle (36±4 °) by toe-off. As in *I. iguana*, flexion at the metatarso-phalangeal joint raises the heel off the ground and raises the distal tibia relative to its proximal end, leading to continued anterior inclination of the tibia throughout the step (maximum 93±3 °) that reflects axial rotation of the femur. Later in stance, the tibia becomes aligned more closely with the sagittal plane as the knee is extended. The femur retracts through an arc of at least 90 ° through stance.

Ground reaction forces and limb orientation

The ground reaction force is oriented posteriorly when the foot is placed on the ground and shifts anteriorly through stance (Fig. 6), reflecting initial deceleration of the animal at foot contact, followed by reacceleration as the foot pushes off the substratum (e.g. Alexander, 1977; Cavagna et al., 1977). The ground reaction force is also oriented medially at the beginning of the step in *I. iguana* (Fig. 6). However, the vertical component of the ground reaction force increases much more rapidly than the medial component through stance, with medial component magnitude averaging less than 15 % of vertical component magnitude by midstep. As a result, the medial inclination of the ground reaction force decreases considerably through the first 10–15 % of the step and averages only 8±7 ° when peak limb bone stress is developed near midstep. In *A. mississippiensis*, the ground reaction force often is oriented slightly laterally at the start of the step and can remain so at peak stress; however, this inclination is very small (3±7 °), indicating an essentially vertical force. Both vertical and medial components of the ground reaction force reach maxima near midstep.

Changes in limb position and the direction of the ground reaction force are similar in both species, indicating that their limb bones encounter similar loading regimes during stance (Fig. 6). Through the step, as the tibia becomes aligned

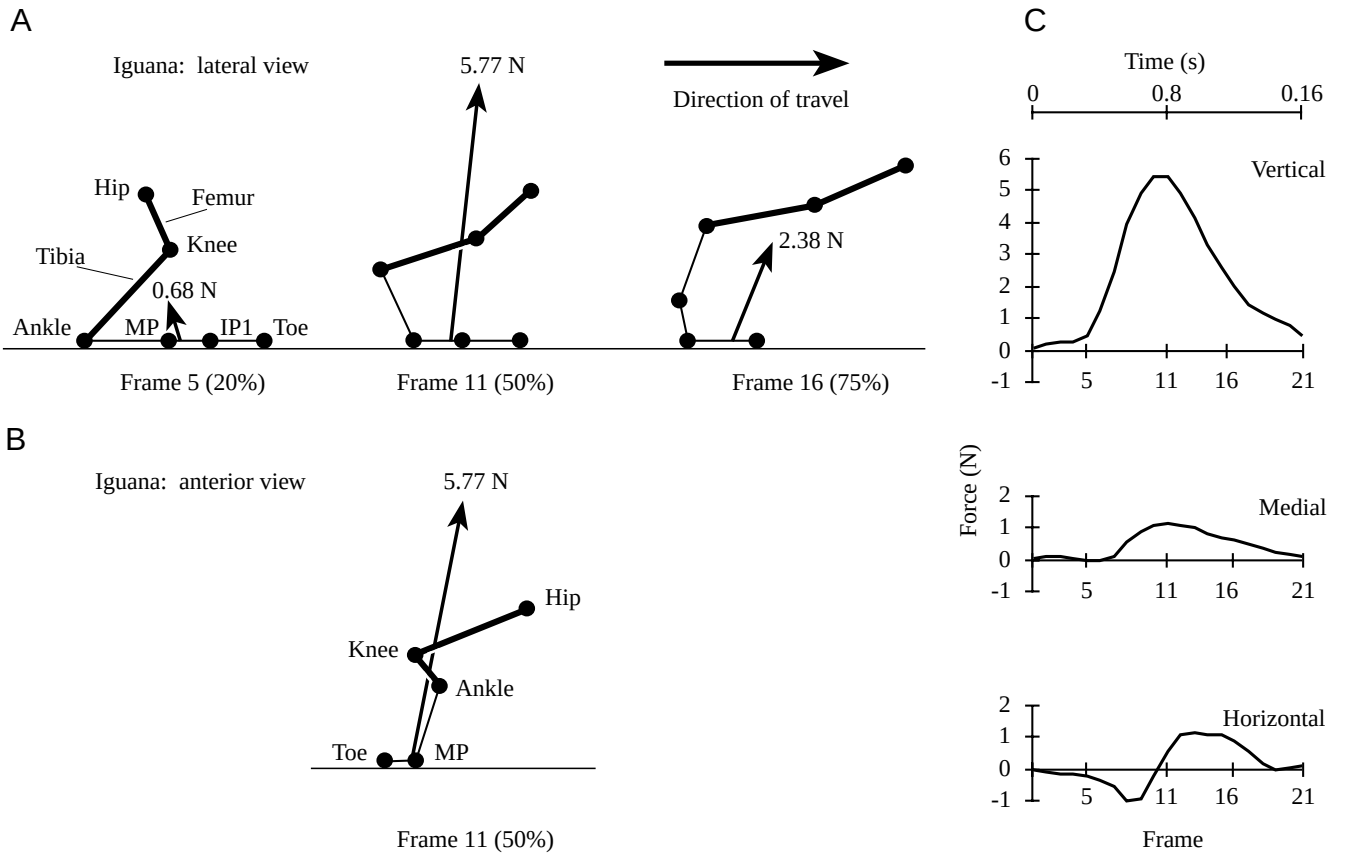

Fig. 6. Limb segment positions at points in the representative step from *Iguana iguana* illustrated in Fig. 5, with the direction and magnitude of the ground reaction force vector illustrated. (A) Right lateral view. Segment positions traced from video. (B) Anterior view. Segment positions calculated from kinematic data. In A and B, the femur and tibia are highlighted by bold lines. (C) Vertical, medial and horizontal components of the ground reaction force during the illustrated step. Positive forces are upwards, medial and anterior, respectively (in the absolute frame of reference). MP, metatarso-phalangeal joint; IP1, first interphalangeal joint. The positions of interphalangeal joints other than IP1 have been omitted for clarity.

essentially parallel to the ground and the ground reaction force shifts more vertically, the angle between the two (from the distal end of the bone) increases, reaching 62±6 ° in *A. mississippiensis* and 74±17 ° in *I. iguana* at peak stress. Thus, in spite of the near-vertical orientation of the ground reaction force at midstep, the kinematics of these species result in a large component of the reaction force acting normal to the tibia (‘posteromedially’ in the anatomical frame of reference), indicating substantial bending loads. Peak forces normal to the tibia in these species are usually approximately equal to or slightly greater in magnitude than forces acting along the tibial axis. In addition, the lateral deflection of the foot, combined with an essentially vertical ground reaction force, suggests that the ground reaction force will usually act lateral to the axis of the lower leg.

In both species, the femur begins the step directed anteriorly and subhorizontally. While the femur is retracted through the step (i.e. the knee moves posteriorly with respect to the hip), the hip is also moving forwards. The femur therefore passes over the foot and, thus, over the point from which the ground reaction force originates. As the inclination of the ground reaction force shifts anteriorly through the step and becomes more vertically directed, the angle between it and the femur generally decreases until midstep, but then increases as the leg is further extended until toe-off (Fig. 6). Thus, in contrast to the tibia, the femur is often most closely aligned with the ground reaction force at peak stress. Nonetheless, this angle is large in both species (*A. mississippiensis*, 38±7 °; *I. iguana*, 40±16 °). As for the tibia, the magnitudes of ground reaction force components acting transverse to the femur roughly equal those acting along the axis of the femur for much of the step in both species, suggesting that the femur also experiences substantial bending. This bending is initially directed ‘dorsoventrally’; however, as the femur rotates about its long axis, the ground reaction force (directed almost vertically for most of the step) comes to act closer to the anatomical ‘anteroposterior’ direction. In addition, despite the anterior shift in the orientation of the ground reaction force through stance, forward movement of the hip causes the line of action of the ground reaction force to act posterior (in an absolute frame of reference) to the femur for much of the step, including the time of peak stress.

Moments exerted by the ground reaction force

In both species, the ground reaction force exerts moments

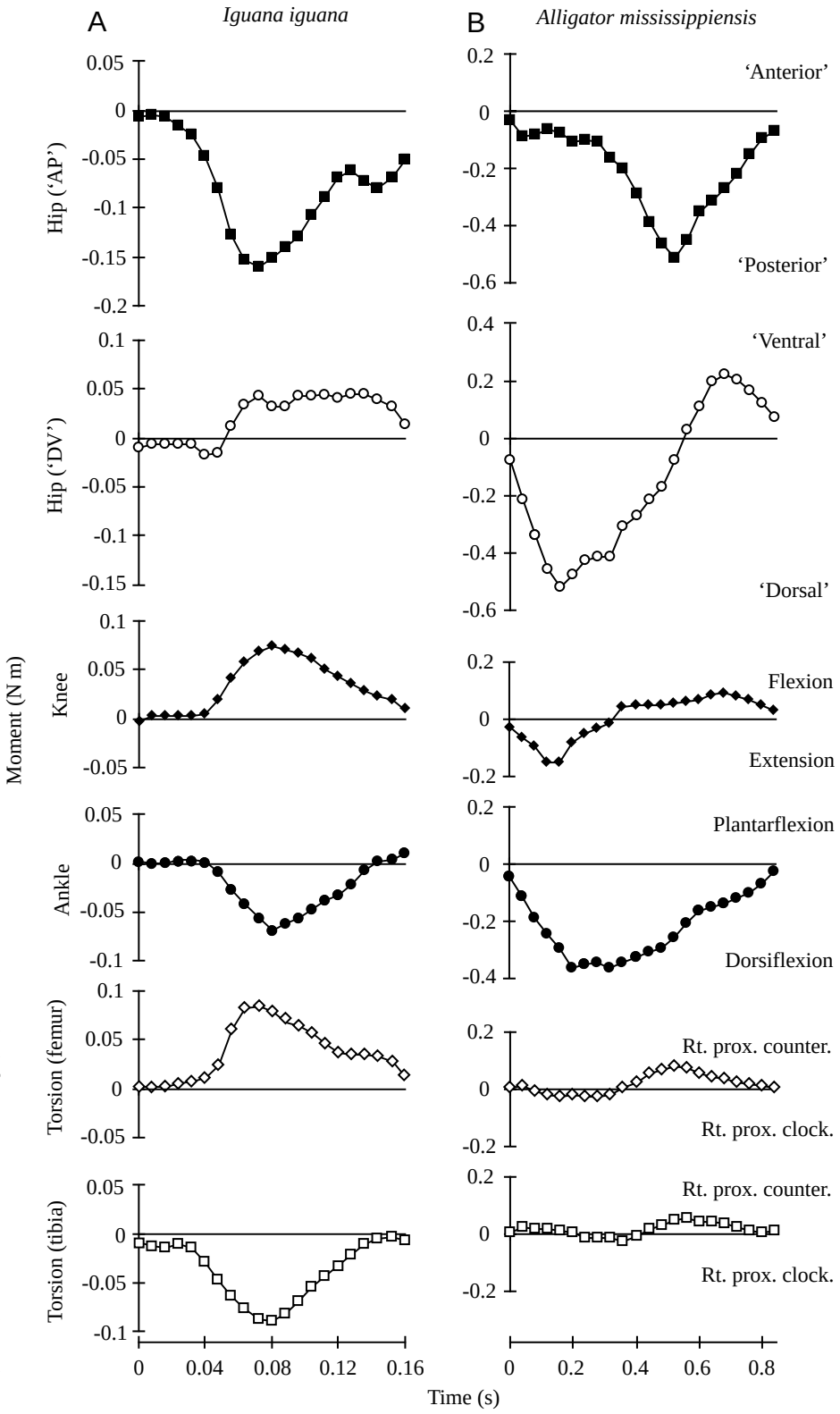

Fig. 7. Moments exerted by the ground reaction force about the hindlimb joints and the long axes of the femur and tibia for representative steps from (A) *Iguana iguana* and (B) *Alligator mississippiensis*. Directions of moments are labeled to the right of the figure. Hip ('AP'), the ground reaction force moment about the hip in the anatomical anterior and posterior directions; Hip ('DV'), the ground reaction force moment about the hip in the anatomical dorsal and ventral directions; Rt. prox. clock., clockwise when viewing the right bone from its proximal end; Rt. prox. counter., counterclockwise when viewing the right bone from its proximal end.

tending to flex (collapse) both the knee and ankle for most of stance (Fig. 7). For equilibrium to be maintained at these joints, the knee and ankle extensor muscles must be active to counteract these moments. Both knee and ankle moments are small at the beginning of stance, when ground reaction force magnitudes are low. The moments at both joints increase as the ground reaction force magnitudes increase towards midstep, but then decline as ground reaction force magnitudes decrease towards the end of the step (Fig. 7).

Moments about the hip are most simply described with

reference to the two anatomical planes of the femur defined in Fig. 1. With few exceptions, the ground reaction force exerts a moment at the hip that tends to rotate the femur 'posteriorly' about the axis of the anatomical 'anteroposterior' plane throughout stance (Fig. 7). However, through the step, axial rotation of the femur and elevation of the heel off the substratum shift the 'anteroposterior' plane so that its 'anterior' surface comes to face ventrally in an absolute frame of reference. Thus, after a 90 ° rotation, a 'posterior' moment would be a tendency to rotate the femur upwards (dorsally) in an absolute frame of reference (Fig. 1). The magnitude of this moment generally increases until midstep, after which it steadily decreases (Fig. 7). With respect to the anatomical 'dorsoventral' plane, the ground reaction force initially exerts an 'abductor' moment (i.e. it rotates the distal end of the femur dorsally relative to its proximal end: Fig. 7). However, as the femur rotates about its long axis and the hip moves forwards through the step, this 'abductor' moment reaches a maximum early in the step, then decreases to zero and increases in the opposite direction, becoming an 'adductor' moment tending to rotate the femur 'ventrally' (Fig. 7). After 90 ° axial rotation of the femur, such a tendency to rotate the femur 'ventrally' would equal a tendency to rotate the femur posteriorly (backwards) in an absolute frame of reference (Fig. 1). Further, it indicates that hip abductor muscles, rather than adductors, must be activated late in stance to counter this moment.

The ground reaction force also exerts torsional moments about the long axes of the femur and tibia (Fig. 7). As stance begins, the ground reaction force often briefly acts anterior to the femur, producing torsional moments that tend to rotate the femur posteriorly (i.e. rotate the right femur clockwise if viewed from its proximal end). However, as the femur retracts and the hip moves forward, much larger, anteromedial torsional moments develop (tending to rotate the right femur counterclockwise if viewed from its proximal end) that peak after midstep (Fig. 7). Torsional moments for the tibia were more variable; however, for 19 of the 26 trials in *I. iguana* (73 %), the greatest torsional moments indicated lateral rotation of the tibia (clockwise looking down on the proximal end of a vertically oriented right tibia: Fig. 7). Two of the six trials for *A. mississippiensis* exhibited similar tibial torsion, although the other four showed medially directed torsional moments.

Hindlimb muscle forces

Because of the large moments exerted by the ground reaction force about the hindlimb joints, hindlimb muscle forces are also large and make substantial contributions to axial and bending stress in the femur and tibia of *I. iguana* and *A. mississippiensis*. The bending moments induced by the limb muscles usually exceed those induced by the components of the ground reaction force acting transverse to the limb (Fig. 8). For example, the knee extensors originate on the ilium (iliotibialis) and on the 'dorsal' femur (femorotibialis); forces exerted by these muscles bend the distal end of the femur dorsally towards the proximal end, placing its 'dorsal' aspect in compression. Hip adductors act in an opposite fashion, bending the distal femur ventrally and placing the 'dorsal' surface in tension. Because the line of action of the adductors is at a greater net angle to the long axis of the femur than the line of action of the knee extensors (Fig. 3; Table 1), a relatively greater component of adductor force than of knee extensor force acts transverse to the femur. However, the knee extensors must exert force to counter not only the flexor moment of the ground reaction force but also flexor moments produced by the ankle extensors and hip adductors that span the knee. Further, adductor force tends to decrease by midstep as the femur rotates about its long axis and the ground reaction force comes to generate an 'adductor' moment itself. As a result of these factors, and the long moment arm of the adductors at the hip compared with that of the knee extensors at the knee, peak knee extensor forces can be 4–6 times greater than peak adductor forces. Consequently, muscles spanning the length of the femur generate a large net bending moment that places the 'dorsal' cortex in compression (Fig. 8). At the beginning of the step, bending moments due to the ground reaction force also bend the femur 'dorsally' and the muscular and external moments are additive. Through the step, however, axial rotation of the femur causes the ground reaction force bending moment to change direction and bend the femur 'ventrally'. Nonetheless, because the knee extensors must still counter a large flexor moment at the knee, they continue to exert substantial force and produce a bending moment that exceeds that due to the ground reaction force. Muscular forces thus act to maintain a 'dorsally' directed bending moment throughout stance.

The effects of joint moments on hindlimb muscle forces are also pronounced at the ankle and knee, where muscular moment arms are smaller than at the hip, and the ankle and knee extensor muscles must exert large forces to prevent the ground reaction force from collapsing these joints (Fig. 8). At the ankle, because of the plantigrade foot posture and long feet of *I. iguana* and *A. mississippiensis*, the ground reaction force has a long moment arm about the joint and can produce a large flexor torque. The ankle extensors, with lines of action very close to the ankle joint, have shorter moment arms about the ankle than the ground reaction force and, thus, must exert a collective force much larger than the ground reaction force to prevent joint collapse. As a result of the large forces the extensors must exert, and of the curvature of the tibia (which bows the bone 'laterally' and displaces its centroid from the muscular line of action), the ankle extensors induce a large bending moment about the tibial midshaft that places the 'lateral' (dorsiflexor) surface in tension and the 'medial' (plantarflexor) surface in compression. This moment surpasses that caused by the ground reaction force (often by a factor of two or more), but bends the bone in the same direction. In contrast, no muscles bend the tibia in the 'anteroposterior' direction. Although bending moments due to the ground reaction force in the 'anteroposterior' and 'mediolateral' directions are usually similar in magnitude, the large

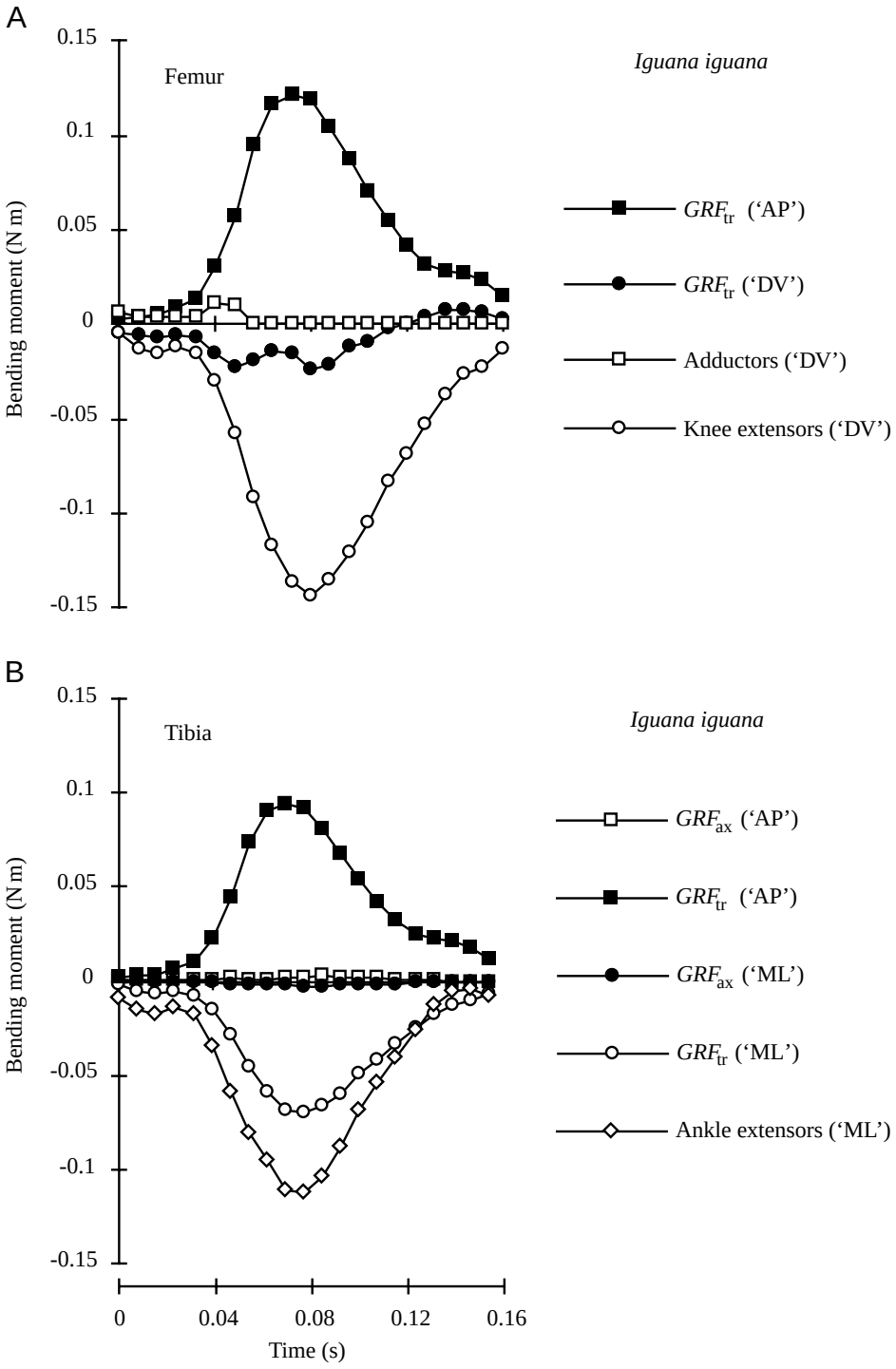

Fig. 8. Comparison of bending moments exerted in the femur (A) and tibia (B) of *Iguana iguana* by muscle forces and components of the ground reaction force. Anatomical directions in which moments act are indicated as: 'AP', anteroposterior; 'DV', dorsoventral (femur); 'ML', mediolateral (tibia). GRF_{ax}, the bending moment exerted by the axial component of the ground reaction force due to bone curvature in the direction indicated; GRF_{tr}, the bending moment exerted by the component of the ground reaction force acting transverse to the bone in the direction indicated; Ankle extensors, Adductors, Knee extensors, the bending moments exerted by these muscle groups in the directions indicated. Sign conventions: Femur 'AP', positive is bending to place the 'anterior' surface in tension, the 'posterior' surface in compression; Femur 'DV', negative is bending to place the 'ventral' surface in tension, the 'dorsal' surface in compression; Tibia 'AP', positive is bending to place the 'anterior' surface in tension, the 'posterior' surface in compression; Tibia 'ML', negative is bending to place the 'lateral' surface in tension, the 'medial' surface in compression. Bending moments applied to the femur by the axial component of the ground reaction force (due to bone curvature) are very small and have been omitted for clarity.

'mediolateral' bending moment produced by the ankle extensors deflects the axis of tibial bending closer to the 'mediolateral' plane.

Femoral and tibial stresses

Stress calculations for the femur of *I. iguana* and *A. mississippiensis* confirm that it is loaded in a combination of axial compression, bending and torsion in both species (Table 3). In both species, the 'posterodorsal' cortex of the femur is placed in compression whereas the 'anteroventral' cortex is placed in tension (Fig. 9). The direction of femoral bending changes little for the first two-thirds (or more) of stance, with the neutral axis typically oriented 30–40 ° from the anatomical 'anteroposterior' axis. Later in stance, neutral axis orientation gradually shifts, keeping the net direction of bending closer to dorsoventral (in an absolute frame of reference) by tracking axial rotation of the femur and rotating towards the anatomical 'dorsoventral' axis (Fig. 9). Axial compression is superimposed on bending in the femur of both species (–2.4±0.4 MPa in *A. mississippiensis*, –4.9±2.0 MPa in *I.*

Table 3. *Mean peak stresses and safety factors calculated from force platform data for the femur and tibia of* Iguana iguana *and* Alligator mississippiensis

	Peak stress (MPa)				Neutral axis angle from AP (degrees)	Safety factor in bending	
	Tensile	Compressive	Axial	Shear		Mean	Worst case
Iguana iguana (*N*=26)							
Femur	+27.1±10.8	−37.0±14.2	−4.9±2.0	5.8±2.8 (*N*=24)	30.5±19.0	8.0	4.5
Tibia	+43.1±18.8	−18.6±8.5	−5.2±2.7	2.6±1.3 (*N*=19)	2.2±1.4	5.1	2.7
Alligator mississippiensis (*N*=6)							
Femur	+11.7±1.5	−16.4±2.2	−2.4±0.4	1.9±0.5 (*N*=6)	36.9±11.7	6.7	3.2
Tibia	+28.8±4.3	−10.9±1.7	−2.3±0.5*	0.7±0.3 (*N*=2)	3.0±0.8	2.7	1.3

Shear stresses are reported for counterclockwise rotation of the right femur and clockwise rotation of the right tibia, both bones viewed from their proximal end (sample sizes in parentheses); for all other other variables, *N*=26 for *Iguana iguana* and *N*=6 for *Alligator mississippiensis*.

Deviations of the neutral axis from the 'anteroposterior' (AP) axis of each bone are clockwise.

See text for details of mean and worst-case safety factor calculations.

*For the tibia, the axial stress reported is that applied to the entire crus.

Values are means ± S.D.

iguana); thus, peak compressive stresses are greater than peak tensile stresses (Fig. 9). Peak femoral stress was not significantly correlated with speed in either species or with gait in *I. iguana* (non-parametric Kruskal–Wallis test). However, mean peak stresses in the femur of *I. iguana* (+27.1±10.8 MPa 'anteroventral', −37.0±14.2 MPa 'posterodorsal') were significantly higher than those in *A. mississippiensis* (+11.7±1.5 MPa 'anteroventral', −16.4±2.2 MPa 'posterodorsal') (P<0.001 for both comparisons; Table 3).

In both *I. iguana* and *A. mississippiensis*, the tibia is loaded in bending, with the 'lateral' (dorsiflexor) surface in tension and the 'medial' (plantarflexor) surface in compression (Table 3; Fig. 9). The neutral axis is aligned close to the anatomical 'anteroposterior' plane for almost all of stance, although a slight 'anterolateral–posteromedial' inclination (5–10 °) increases at the end of the step. Axial compression is superimposed on tibial bending in both species (−2.3±0.5 MPa in *A. mississippiensis*, −5.2±2.7 MPa in *I. iguana*). However, the fibula shifts the neutral axis of crural bending to place the tibia in net tension (i.e. peak tension exceeds peak compression) (Figs 4, 9). Peak stresses are lower in *A. mississippiensis* (+28.8±4.3 MPa 'anterolateral', −10.9±1.7 MPa 'posteromedial') than in *I. iguana* (+43.1±18.8 MPa 'anteroventral', −18.6±8.5 MPa 'posterodorsal'), but only peak compression differs significantly (P=0.016; Table 3). For both species, mean peak tensile stresses in the tibia are significantly greater than mean peak tensile stresses in the femur (non-parametric paired sign tests, P<0.001 for *I. iguana*, P=0.031 for *A. mississippiensis*).

Shear stresses in the femur due to the ground reaction force average 1.9±0.5 MPa in *A. mississippiensis* and 5.8±2.8 MPa in *I. iguana* (Table 3). In the tibia, shear stresses (for steps exhibiting clockwise torsion of the tibia, viewed from its proximal end) averaged 0.7±0.3 MPa in *A. mississippiensis* and 2.6±1.3 MPa in *I. iguana*. As noted in the Materials and methods section, these values are minimum estimates that do not account for torsion induced by the limb muscles.

Safety factor calculations

'Mean' safety factors in bending for the femur and tibia in *I. iguana* are 8.0 and 5.1, respectively (Table 3). These decrease to 4.5 (femur) and 2.7 (tibia) in the 'worst-case' estimates. For *A. mississippiensis*, 'mean' safety factors in bending for the femur and tibia are 6.7 and 2.7, respectively, and 'worst-case' estimates decrease to 3.2 (femur) and 1.3 (tibia) (Table 3). Safety factors in shear were not calculated because of the uncertainties in shear stress estimates from the force platform data.

Correlations of stress magnitudes with limb posture in I. iguana

Peak tensile and peak compressive stresses in the femur both tend to be higher during upright steps in *I. iguana* (Table 4). Stresses on the 'anterior' and 'dorsal' femoral cortices (at the time of overall peak stress) are also correlated with femoral posture: 'anterior' stress decreases significantly with more upright posture, whereas 'dorsal' stress increases significantly in more upright steps (Table 4). These trends are consistent with observations from *A. mississippiensis* in limb bone strain experiments (Blob and Biewener, 1999), verifying that tests of the alternative mechanisms proposed to explain these loading patterns (see Materials and methods) are warranted.

Axial stress (at the time of overall peak stress) shows a significant trend to be higher among more upright steps (Table 4). However, neither the moment arm of the ground reaction force about the hip, nor the force exerted by the adductor muscles, is significantly correlated with femoral posture (Table 4). Instead, knee extensor force increases significantly among more upright steps (Table 4; Fig. 10). Besides adductor force (which did not change significantly with limb posture), both the ground reaction force and the

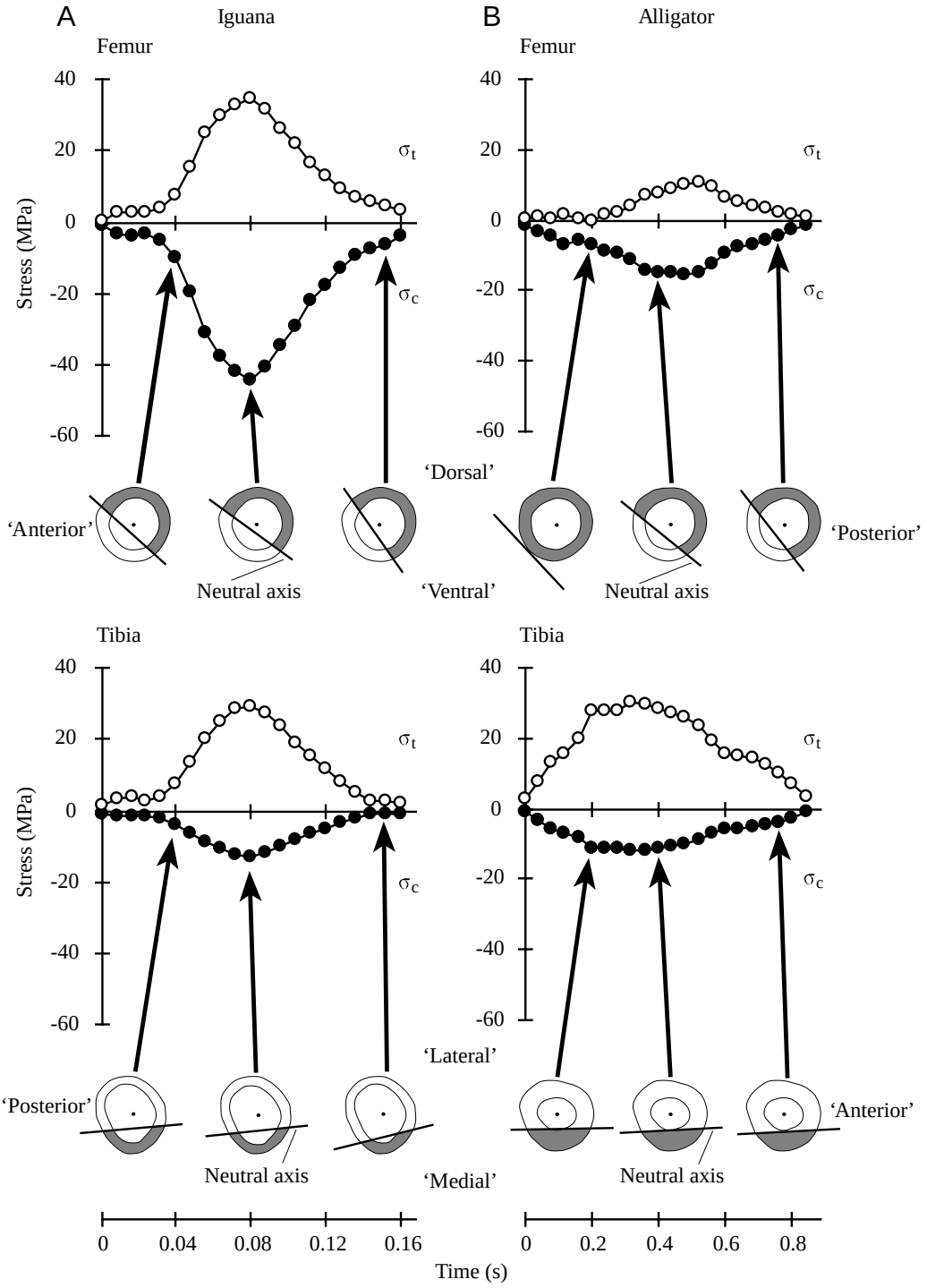

Fig. 9. Maximum tensile (σ_t, open circles) and compressive (σ_c, filled circles) stresses calculated to act in the femur and tibia through representative steps in (A) *Iguana iguana* and (B) *Alligator mississippiensis*. Cross sections below each trace illustrate the position and orientation of the neutral axis for the frames indicated by the arrows. Shading indicates the portion of the cross section that experiences compression.

ankle extensors can potentially contribute to the flexor moment at the knee and, thus, require the knee extensors to exert higher countering forces. Neither the net ground reaction force nor its moment arm at the knee increased significantly among more upright steps (Table 4). However, ankle extensor force is significantly greater in more upright steps (Table 4; Fig. 10) because of increases in ankle joint moment (Table 4). The increase in ankle moment results from an increase in the moment arm of the ground reaction force about the ankle (i.e. the moment arm of the force that the ankle extensors must counter to maintain equilibrium) (Table 4; Fig. 10) that is probably related to earlier lifting of the ankle from the substratum in more upright steps. Maximum metatarso-phalangeal flexion occurs earlier in upright steps (Table 4), shifting the origin of the ground reaction force further anteriorly along the foot at peak stress and increasing its moment arm and the joint moment at the ankle during upright locomotion (Fig. 10).

Table 4. *Results of regressions of stress, force and kinematic variables on femoral posture (angular deviation of the femur from horizontal, in degrees) for* Iguana iguana

Variable	RMA slope	r^2	P
σ_t (maximum) (MPa)	1.036	0.131	0.069
σ_c (maximum) (MPa)	–1.372	0.174	0.034*
σ_t (anterior) (MPa)	–0.736	0.199	0.022*
σ_c (dorsal) (MPa)	–1.446	0.304	0.004*
σ_c (axial) (MPa)	–0.188	0.276	0.006*
GRF_{net} (N)	NS	0.066	0.207
R_{hip} (mm)	NS	0.002	0.821
R_{knee} (mm)	NS	0.016	0.535
R_{ankle} (mm)	0.527	0.280	0.005*
Mom_{ank} (Nm)	0.004	0.249	0.001*
F_m (adductors) (N)	NS	0.024	0.448
F_m (knee extensors) (N)	1.007	0.204	0.021*
F_m (ankle extensors) (N)	1.549	0.298	0.004*
$Apex_{mp}$ (degrees)	–0.553	0.219	0.016*

Reduced major axis (RMA) slopes are reported for regressions significant (*) at $P<0.05$; $N=26$ for all regressions.

σ_t, tensile stress; σ_c, compressive stress; GRF_{net}, magnitude of the net ground reaction force vector; R, moment arm of the *GRF* about the limb joint; Mom_{ank}, ankle joint moment; F_m, force exerted by a muscle group; $Apex_{mp}$, arcsine-transformed (Sokal and Rohlf, 1995) fraction of time through the step when metatarso-phalangeal flexion reaches its apex; NS, not significant.

For variables positive in sign (σ_t, GRF_{net}, R, F_m, Mom_{ank}, $Apex_{mp}$), positive slopes indicate increasing values with more upright posture.

Compressive stresses (σ_c) are negative, so negative slopes indicate increasing deviation from zero with more upright posture.

Discussion

Limb bone loading in Iguana iguana *and* Alligator mississippiensis

Analyses of locomotor forces and kinematics in *I. iguana* and *A. mississippiensis* generally confirm interpretations of loading regimes in the femur and tibia of these species derived from *in vivo* bone strain data (Blob and Biewener, 1999). In both species, the femur and tibia experience a combination of bending and torsion. For the femur in particular, the ground reaction force appears to augment the torsional moment applied by the caudofemoralis for most of stance, suggesting that shear stress is substantial. Although a few studies have noted substantial torsion in vertebrate limb bones during terrestrial locomotion (e.g. Keller and Spengler, 1989; Carrano, 1998), in most mammals and birds, bending and axial compression are much greater than shear (Lanyon and Smith, 1970; Rubin and Lanyon, 1982; Rubin and Lanyon, 1984; Biewener, 1983a; Biewener et al., 1983; Biewener et al., 1988). Thus, together with previous recordings of high shear strains (Blob and Biewener, 1999), the strong indications of limb bone torsion in saurians from ground reaction force data point to a major transition in limb bone loading through the evolutionary history of amniotes.

What factors contribute to the differences in bone loading observed between *I. iguana* and *A. mississippiensis* and other taxa? In both *I. iguana* and *A. mississippiensis*, the mediolateral component of the ground reaction force is small relative to the vertical component and the net ground reaction force is usually oriented less than 10° from vertical at peak stress. A similar orientation is observed in other species using non-parasagittal locomotion, including varanid lizards (Christian, 1995) and turtles (Jayes and Alexander, 1980), as well as in species that use parasagittal locomotion, such as horses (Biewener et al., 1983; Biewener et al., 1988) and other mammals (A. Biewener, unpublished data). If the orientation of the ground reaction force is similar in reptiles and mammals, then differences in limb bone loading patterns between non-parasagittal and parasagittal locomotion must be caused, instead, by differences in limb posture and kinematics. The non-parasagittal kinematics of *I. iguana* and *A. mississippiensis* place the tibia and femur at large angles to the ground reaction force at peak stress: as a result, components of the ground reaction force acting normal to the limb bones often equal or exceed components acting along the axes of the bones, producing substantial bending moments. Large force components normal to bone axes have been found to bend the limb bones of small mammals that use highly crouched postures (Biewener, 1983a). However, in large mammals with a more upright posture and parasagittal kinematics, bending moments due to axial forces (acting about the moment arm as a result of bone curvature) are typically more important than those due to transverse forces (Biewener et al., 1983; Biewener et al., 1988). With respect to bone torsion, in both *I. iguana* and *A. mississippiensis*, the femur has a large lateral arc of retraction and the tibia is inclined laterally through much of stance, placing the line of action of the ground reaction force at a sizable distance from the long axes of both bones. As a result of these large torsional moment arms, substantial torsional moments are produced about these elements in both species. In contrast, in both large and small mammals with parasagittal posture, the line of action of the ground reaction force is aligned much more closely with the long axes of the limb bones (Biewener et al., 1983; Biewener et al., 1988), reducing its rotational moment arm and, thereby, the torsional moment it can exert.

The most notable disparity between the results of bone stress and *in vivo* bone strain analyses is in the interpretation of the loading regime for the alligator tibia. Although stress calculations indicate that the alligator tibia is loaded in net tension because the presence of the fibula displaces the neutral axis of the crus as a whole, *in vivo* strain measurements (Blob and Biewener, 1999) indicated that the alligator tibia was loaded in net compression. Overestimation of the effects of the fibula in stress calculations for *A. mississippiensis* could contribute to this discrepancy. Correction factors to account for fibular load-bearing in tibial stress calculations were based on measurements from an articulated iguana crus (see Materials and methods). However, the tibia of *A. mississippiensis* appears to be relatively more robust than that of *I. iguana* (Fig. 9), with relatively greater second moments of area and

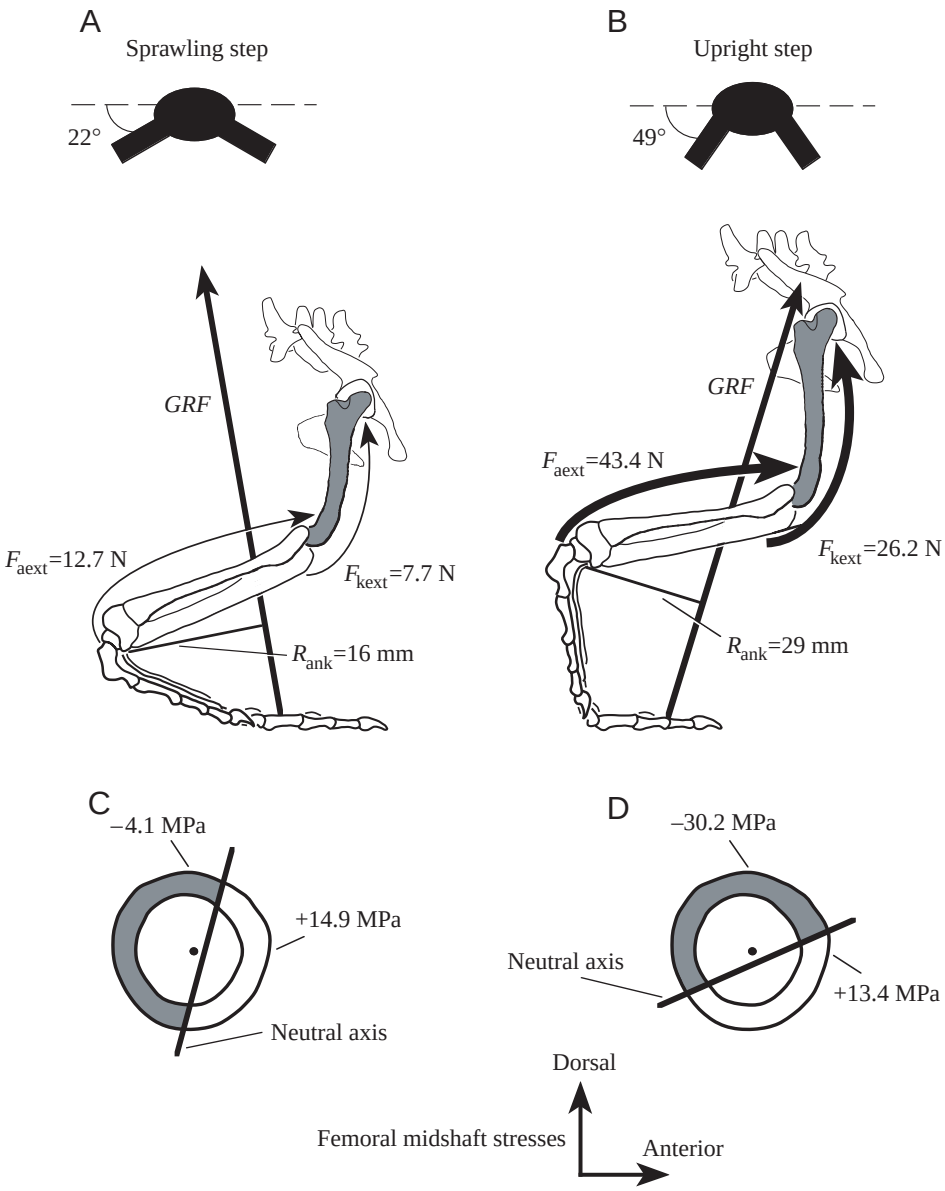

Fig. 10. Changes in muscle forces, the moment arm of the ground reaction force about the ankle (R_{ank}) and femoral stress as a more upright femoral posture is used by *Iguana iguana*. Force, moment arm and stress values and limb bone positions are based on data from representative sprawling (A,C) and more upright (B,D) steps at the time of peak femoral stress. Sketches filled in black at the top of A and B illustrate femoral depression from the horizontal (dashed line) for each step. The kinematic positions of the limb bones are illustrated in right lateral view in A and B; the femur is shaded, and the direction of travel is to the right. Force vector lengths are drawn to reflect the lines of action of muscle groups and the ground reaction force (*GRF*). R_{ank} is greater in more upright steps (B), causing the ankle extensor muscles to exert greater force (F_{aext}) to maintain rotational equilibrium at the ankle. As a result, the knee extensor muscles must exert greater force (F_{kext}) to maintain rotational equilibrium at the knee during upright steps. Greater vector thicknesses in B reflect these increases in muscle force during more upright steps. Note that, in the sketches of the hindlimb skeleton, the proximal end of the femur recedes into the page; thus, from the lateral perspective illustrated, apparent differences in the moment arm of the *GRF* about the knee and hip are greatly exaggerated. (C,D) Posture-related changes in stress illustrated for femoral midshaft cross sections. Stress magnitudes on the 'dorsal' and 'anterior' cortices are labeled for each section. Bold straight lines through cross sections indicate the neutral axis of bending (where stress is zero), which separates portions of the bone loaded in compression (shaded) from portions loaded in tension (unshaded); the direction of bending is perpendicular to this axis. Increases in knee extensor force lead to greater (more negative) 'dorsal' bending stresses during more upright locomotion (D). However, increases in axial compression during upright steps cause decreases in tensile stress on the 'anterior' cortex of the femur during more upright locomotion (D).

cross-sectional area. It is possible, therefore, that deflection of the neutral axis is not as great in *A. mississippiensis* as in *I. iguana* and that the effects of the fibula were overestimated for *A. mississippiensis*. Nevertheless, this difficulty applies predominantly to calculations of load magnitudes and does not affect interpretations of which bone cortices are placed in tension and compression.

Limb bone safety factor in A. mississippiensis *and* I. iguana

'Mean' safety factors in bending for the femur and tibia of *I. iguana* and *A. mississippiensis* based on force/video analyses were generally lower than safety factors for the same elements calculated from *in vivo* strain data (Blob and Biewener, 1999). An exception was the femur of *A. mississippiensis*, for which force/video-based safety factors were 6% higher than strain-based safety factors. However, for the other three elements, strain-based safety factors were greater by 12% (iguana tibia), 35% (iguana femur) and 102% (alligator tibia). Similar discrepancies between force/film- and strain-based calculations of load magnitudes have been recognized in previous studies (Biewener et al., 1983). In the horse metacarpus and radius, for example, peak stress calculations based on measured external joint moments were 1.5–4 times higher than calculations based on *in vivo* strain recordings

(Biewener et al., 1983). Inaccurate assumptions about the orientation and activity of muscles crossing the limb joints could contribute to these observed discrepancies (Biewener et al., 1983). Although effort was made to model limb muscle activity in *I. iguana* and *A. mississippiensis* as realistically as possible, the model is inherently limited because information on activity and force development is not available for many limb muscles of these animals. Nonetheless, in the context of previous studies, discrepancies between strain and force/video estimates of load magnitudes in *I. iguana* and *A. mississippiensis* are large only for the alligator tibia.

Although 'mean' force/video-based safety factors are generally lower than strain-based safety factors for *I. iguana* and *A. mississippiensis* limb bones in bending, for three of four bones tested, safety factors in these species are still higher than the values typically ascribed to birds and mammals (Alexander, 1981; Rubin and Lanyon, 1982; Biewener, 1993). Considering the tendency for stress magnitudes to be overestimated and safety factor estimates to be lower in force/film analyses (Biewener, 1983a; Biewener et al., 1983; Biewener et al., 1988), force data from *I. iguana* and *A. mississippiensis* appear to verify the high safety factors calculated from bone strain data (Blob and Biewener, 1999). If the high safety factors for *I. iguana* and *A. mississippiensis* limb bones reflect the broader diversity of taxa within their respective lineages, then high limb bone safety factors might have been ancestral for amniotes, which would suggest that lower safety factors evolved independently in birds and mammals (Blob and Biewener, 1999). However, our bone strain measurements also suggested that safety factors in shear were lower than safety factors in bending for *I. iguana* and *A. mississippiensis* and, thus, might provide a more biologically meaningful index for comparison with other species. Safety factors for shear could not be calculated reliably from the force platform data obtained here. Thus, because it is possible that safety factors in bending might be overestimates of net safety factors for alligator and iguana limb bones, the safety factors calculated from these force/video analyses should be viewed with caution in the context of testing hypotheses about the evolution of skeletal design and bone material properties.

Load magnitudes and limb posture: evolutionary implications

Force-platform data from *I. iguana* show correlations between limb posture and load magnitudes that are consistent with those identified for *A. mississippiensis* during analyses of *in vivo* bone strain: tensile stresses on the 'anterior' cortex of the femur tend to be lower in more upright steps, but compressive stresses on the 'dorsal' surface of the femur tend to be higher in more upright steps. As hypothesized in the bone strain analyses, axial compressive stress is higher in more upright steps, accounting for the decrease in 'anterior' tension with more upright posture. In addition, force platform and kinematic analyses indicate the mechanical basis for changes in 'dorsoventral' stress. Rather than being mediated by changes in adductor force, increases in 'dorsoventral' bending stress of the femur are correlated with a cascade of events originating at the foot and ankle (Fig. 10). Flexion at the metatarsophalangeal joint reaches its apex relatively earlier in upright steps. This indicates that the ankle is raised off the substratum earlier in more upright locomotion, shifting the origin of the ground reaction force further (anteriorly) from the ankle at the time of peak stress. Increases in the moment arm of the ground reaction force at the ankle during more upright locomotion lead to increases in forces exerted by the knee and ankle extensors (Fig. 10). The ankle extensors must exert higher forces to counter the larger ankle flexor moment during more upright steps, causing them to make a greater contribution to the flexor moment at the knee. The knee extensors must exert a greater force to counter this moment, and thus apply a greater bending moment to the femur, increasing compressive strains on its 'dorsal' surface (Fig. 10).

Increases in femoral loads are correlated with the use of upright limb posture in both alligators and iguanas, two species that use broadly similar limb kinematics but represent different phylogenetic lineages (archosaurs and lepidosaurs). This suggests that increased femoral stress, at least at some cortical locations, might be a common feature of postural changes by individuals of species that move their limbs predominantly outside parasagittal planes. This pattern contrasts with that observed during size-related, evolutionary shifts in posture among mammals with near-parasagittal kinematics, in which shifts from a crouched to an upright stance have been demonstrated to mitigate increases in bone loading and maintain bone stresses nearly constant as body size increases (Biewener, 1983a; Biewener, 1989; Biewener, 1990). These conclusions must be regarded as preliminary because they are based on comparative data from only two saurian species from non-avian lineages. However, if posture-related increases in limb bone stress are typical of taxa that use non-parasagittal limb kinematics, then lineages that underwent evolutionary shifts from a sprawling to an upright posture would probably have had to contend with increased limb bone stress through this transition. Limb bone stress increases seem particularly likely for lineages such as crocodilians (Parrish, 1987) and the therapsid ancestors of modern mammals (Schaeffer, 1941a; Schaeffer, 1941b; Jenkins, 1971b; Kemp, 1980; Kemp, 1985; Hopson, 1995) that retained the elongate feet and plantigrade foot posture that facilitate posture-related changes in ankle mechanical advantage (Fig. 10).

The potential magnitudes of evolutionary, posture-related increases in limb bone stress are difficult to evaluate (Blob, 2001). Although femoral posture is significantly correlated with femoral stress patterns, it is not a strong predictor of bone stress magnitude (r^2<0.31 for regressions of stress on posture; Table 4). Limb bone strength in fossil therapsids and crocodilians, if similar to values in extant amniotes (e.g. Biewener, 1982; Lanyon and Rubin, 1985; Currey, 1987), might well have been adequate to accommodate increases in locomotor stress. Furthermore, the maintenance of axial rotation of the femur by crocodilians using the high-walk (Cott, 1961; Brinkman, 1980b; Gatesy, 1991; Blob and Biewener, 1999) demonstrates that dramatic kinematic changes (e.g.

elimination of femoral torsion) need not accompany the use of a more upright stance. However, it is noteworthy that as the lizard *Dipsosaurus dorsalis* grows in size it tends to use a more sprawling locomotor posture (Irschick and Jayne, 2000). In the context of the results from this study, the use of a sprawling posture by larger lizards might help to mitigate size-related increases in limb bone loading. Conversely, a habitually upright limb posture evolved among derived therapsids and primitive mammals that were considerably smaller than their sprawling ancestors (Jenkins, 1971b; Jenkins and Parrington, 1976; Kemp, 1980; Kemp, 1982; Kemp, 1985; Hopson, 1991; Hopson, 1994). This suggests the possibility that increases in limb bone stress related to upright stance could have contributed to the evolution of upright posture at small size in mammals. At what point safety factors typical of modern mammals were achieved, however, remains uncertain.

Appendix

Calculation of muscle forces acting on the femur

In the 'anteroposterior' direction, electrical stimulation and electromyographic data suggest that the caudofemoralis acts as the primary femoral retractor in lizards (Snyder, 1962; Reilly, 1994/95) and alligators (Gatesy, 1997). Other potential retractors (e.g. the iliofibularis) are inactive until the end of stance or the beginning of the swing phase (Jayne et al., 1990; Gatesy, 1997). In both lizards and crocodilians, a thin auxiliary tendon from the caudofemoralis spans the length of the femur to insert at the knee (Romer, 1922; Romer, 1923; Snyder, 1962; Reilly, 1994/95; Gatesy, 1997). However, in both taxa, the primary insertion of the caudofemoralis is proximal to the femoral midshaft *via* a much stouter tendon to the intertrochanteric fossa (lizards, Reilly, 1994/95) or the fourth trochanter (crocodilians, Romer, 1923; Gatesy, 1990; Gatesy, 1997). Rather than attempting to model the distribution of forces transmitted through these two tendons, caudofemoral forces were assumed to be transmitted only through the primary, proximal tendon. Therefore, 'anteroposterior' bending can be calculated from the ground reaction force alone, using a free body diagram of the distal femur, because no muscles spanning the length of the anterior or posterior femur are active during stance. This model could underestimate 'anteroposterior' femoral bending. However, Reilly (Reilly, 1994/95) has observed in the lizard *Sceloporus clarkii* that, as the femur is retracted, tension in the proximal tendon increases, but the auxiliary tendon slackens and its tension decreases. Thus, as forces and bending moments increase through the step, any error introduced by neglecting the auxiliary tendon will decrease.

Forces bending the femur in the 'dorsoventral' direction are exerted by muscles spanning the hip and knee. Electromyographic data for *Sceloporus clarkii* (Reilly, 1994/95) and *Alligator mississippiensis* (Gatesy, 1997) suggest that four muscles (three in *A. mississippiensis*) adduct the femur in lizards and crocodilians: the adductor femoris, puboischiotibialis, flexor tibialis internus and pubotibialis (absent from crocodilians). These muscles all span the femoral midshaft and, thus, contribute to midshaft stresses, bending the femur 'ventrally'. However, because the ground reaction force produces a flexor moment at the knee for most of stance (Fig. 7), knee extensors on the 'dorsal' aspect of the femur must also be active to bend the femur 'dorsally', the opposite direction to bending induced by the hip adductors. Electromyographic data support the femorotibialis as a knee extensor in both lizards (Reilly, 1994/95) and alligators (Gatesy, 1997). Another large muscle, the iliotibialis, is also positioned to extend the knee. Iliotibialis activity has not been tested in lizards, but it shows sporadic activity during stance in slow walking by alligators and may be recruited more heavily at higher speeds (Gatesy, 1997). Because the animals in this study traveled up to four times faster than those studied by Gatesy (Gatesy, 1997) (see Results), the iliotibialis was considered to be active in knee extension.

In lizards and crocodilians, three stance-phase femoral adductors (the puboischiotibialis, flexor tibialis internus and pubotibialis) cross the knee and, therefore, augment the flexor moment of the ground reaction force. Ankle extensors originating from the distal femur also span the knee and contribute to the knee flexor moment. To maintain knee equilibrium, the iliotibialis and femorotibialis must exert sufficient force to counter the sum of these flexor moments. However, because the iliotibialis crosses the hip and exerts a hip moment opposite to that produced by the adductors, there is no unique solution to calculate the forces produced by these muscle groups. A further complication enters adductor force calculations. If joint equilibrium is to be maintained, the hip adductors would be active only while the ground reaction force produces an 'abductor' moment about the 'dorsoventral' axis of rotation. As outlined in the text, rotation of the femur about its long axis and changes in the orientation of the ground reaction force through the step cause the moment induced by the ground reaction force to change direction, from an 'abductor' moment at the beginning of stance to an 'adductor' moment by the end of stance.

To account for known co-activation of antagonist muscles, the activities of muscle groups spanning the knee and hip were modeled as follows. (i) Muscle groups are assumed to act in the same anatomical plane throughout stance. This is reasonable for the femorotibialis, which originates on the proximal femoral shaft, but is a potential source of error in force calculations for muscles originating from the pelvis (although, even for these muscles, insertions will remain in the same anatomical plane through stance). (ii) The force exerted by hip adductors was calculated as that necessary to maintain equilibrium against the 'abductor' moment of the ground reaction force at the hip and was set equal to zero once the ground reaction force produced an 'adductor' moment. The fraction of adductor force contributing to the flexor moment at the knee then was calculated as being proportional to the cross-sectional area of the adductors spanning this joint. The flexor moment generated by these muscles was calculated as the product of this force and their weighted mean moment arm at

the knee. The abductor moment of iliotibialis at the hip was not considered in these calculations of adductor force; therefore, adductor force is underestimated to some degree. However, because the iliotibialis accounts for only one-quarter of the cross-sectional area (and thus force exerted) of the knee extensors (Table 1), this underestimation is minimized as far as possible. (iii) The knee flexor moment generated by the ankle extensors was calculated as the product of the force they exerted (on the basis of joint equilibrium at the ankle) and their weighted mean moment arm at the knee. (iv) The force of the knee extensors was calculated by dividing the total knee flexor moment (due to the ground reaction force, the biarticular hip adductors and the biarticular ankle extensors) by the weighted mean moment arm of the femorotibialis and iliotibialis at the knee.

Two further assumptions were required. First, the iliotibialis was assumed to act as the abductor muscle countering the moment of the ground reaction force at the hip as it shifts to an 'adductor' torque later in stance. Electromyographic data indicate that other muscles in suitable anatomical positions to act as abductors (e.g. ambiens, iliofemoralis, iliofibularis and puboischiofemoralis internus) are generally inactive until the stance–swing transition or swing phase in lizards and crocodilians (Jayne et al., 1990; Gatesy, 1997). Second, in a few trials, muscle forces calculated for the knee extensors were extremely large and would have resulted in unrealistically high muscle stresses. The maximum isometric stresses of lizard limb muscles are generally slightly greater than 200 kPa (e.g. John-Alder and Bennett, 1987; Marsh, 1988). However, stresses developed when a muscle contracts while being stretched can be up to 75 % greater than maximum isometric stress (Cavagna and Citterio, 1974; Flitney and Hirst, 1978; Harry et al., 1990). As the knee is initially flexed in these animals (see Results), active stretching of knee extensors is likely. Therefore, calculated muscle forces were not permitted to exceed values that would produce muscle stresses greater than 350 kPa, with the assumption that the ligaments of the knee joint would help resist knee flexion if the flexor moment became sufficiently large. Kinematic data (see Results) appear to support this hypothesis, because knee flexion stops and the angle of the knee remains fairly constant for a period near mid-stance.

This study was conducted while the authors were affiliated with the University of Chicago. We are grateful to the following people for advice and manuscript critiques: M. Carrano, B. Chernoff, W. Corning, N. Espinoza, S. Gatesy, J. Hopson, F. Jenkins Jr, D. Konieczynski, M. LaBarbera, E. Maillet, L. Panko, S. Reilly, C. Sidor, J. Socha, J. Walker, M. Westneat, J. Wilson and two anonymous referees. We also thank W. Corning and M. Temaner for writing the kinematic and force analysis software used in this study. For assistance with data collection, we thank J. Alipaz, B. Brand, D. Croft, J. Kohler, H. Larsson, P. Magwene, J. Noor and J. Schwartz. We are also grateful to R. Elsey (Rockefeller Wildlife Refuge) for supplying the alligator, to J. Gilpin for building the animal enclosure and machining force plate components, and to C. Abraczinskas for advice on figures. Thanks also to I. Blob, P. Blob and G. Blob for help with literature translations. This research was supported by the Society of Vertebrate Paleontology Predoctoral Fellowship (R.W.B.) University of Chicago Hinds Fund (R.W.B.) and NSF grants IBN-9520719 (R.W.B.) and IBN-9306793 (A.A.B.). Support for R.W.B. during final manuscript preparation was provided by NIH (NS10813-01, -02) and ONR (N000149910184, to M. Westneat and J. Walker).

References

Alexander, R. McN. (1974). The mechanics of a dog jumping, *Canis familiaris*. *J. Zool., Lond.* **173**, 549–573.

Alexander, R. McN. (1977). Terrestrial locomotion. In *Mechanics and Energetics of Animal Locomotion* (ed. R. McN. Alexander and G. Goldspink), pp. 168–203. London: Chapman & Hall.

Alexander, R. McN. (1981). Factors of safety in the structure of animals. *Sci. Prog.* **67**, 109–130.

Beer, F. P. and Johnston, E. R., Jr (1997). *Vector Mechanics for Engineers: Statics and Dynamics*, sixth edition. Boston, MA: McGraw-Hill.

Biewener, A. A. (1982). Bone strength in small mammals and bipedal birds: do safety factors change with body size? *J. Exp. Biol.* **98**, 289–301.

Biewener, A. A. (1983a). Locomotory stresses in the limb bones of two small mammals: the ground squirrel and chipmunk. *J. Exp. Biol.* **103**, 131–154.

Biewener, A. A. (1983b). Allometry of quadrupedal locomotion: the scaling of duty factor, bone curvature and limb orientation to body size. *J. Exp. Biol.* **105**, 147–171.

Biewener, A. A. (1989). Scaling body support in mammals: limb posture and muscle mechanics. *Science* **245**, 45–48.

Biewener, A. A. (1990). Biomechanics of mammalian terrestrial locomotion. *Science* **250**, 1097–1103.

Biewener, A. A. (1993). Safety factors in bone strength. *Calcif. Tissue Int.* **53** (Suppl. 1), S68–S74.

Biewener, A. A. and Full, R. J. (1992). Force platform and kinematic analysis. In *Biomechanics of Structures: A Practical Approach* (ed. A. A. Biewener), pp. 45–73. New York: Oxford University Press.

Biewener, A. A. and Taylor, C. R. (1986). Bone strain: a determinant of gait and speed? *J. Exp. Biol.* **123**, 383–400.

Biewener, A. A., Thomason, J., Goodship, A. and Lanyon, L. E. (1983). Bone stress in the horse forelimb during locomotion at different gaits: a comparison of two experimental methods. *J. Biomech.* **16**, 565–576.

Biewener, A. A., Thomason, J. and Lanyon, L. E. (1988). Mechanics of locomotion and jumping in the horse (*Equus*): *in vivo* stress in the tibia and metatarsus. *J. Zool., Lond.* **214**, 547–565.

Blob, R. W. (2001). Evolution of hindlimb posture in non-mammalian therapsids: biomechanical tests of paleontological hypotheses. *Paleobiol.* **27**, 14–38.

Blob, R. W. and Biewener, A. A. (1999). *In vivo* locomotor strain in the hindlimb bones of *Alligator mississippiensis* and *Iguana iguana*: implications for the evolution of limb bone safety factor and non-sprawling limb posture. *J. Exp. Biol.* **202**, 1023–1046.

Brinkman, D. (1980a). Structural correlates of tarsal and metatarsal functioning in *Iguana* (Lacertilia; Iguanidae) and other lizards. *Can. J. Zool.* **58**, 277–289.

Brinkman, D. (1980b). The hind limb step cycle of *Caiman sclerops* and the mechanics of the crocodile tarsus and metatarsus. *Can. J. Zool.* **58**, 2187–2200.

Brinkman, D. (1981). The hind limb step cycle of *Iguana* and primitive reptiles. *J. Zool., Lond.* **181**, 91–103.

Carrano, M. T. (1998). Locomotion in non-avian dinosaurs: integrating data from hindlimb kinematics, *in vivo* strains and bone morphology. *Paleobiol.* **24**, 450–469.

Carrier, D. R., Heglund, N. C. and Earls, K. D. (1994). Variable gearing during locomotion in the human musculoskeletal system. *Science* **265**, 651–653.

Cavagna, G. A. and Citterio, G. (1974). Effect of stretching on the elastic characteristics and the contractile component of frog striated muscle. *J. Physiol., Lond.* **239**, 1–14.

Cavagna, G. A., Heglund, N. C. and Taylor, C. R. (1977). Mechanical work in terrestrial locomotion: two basic mechanisms for minimizing energy expenditure. *Am. J. Physiol.* **233**, R243–R261.

Christian, A. (1995). Zur Biomechanik der Lokomotion vierfüßiger Reptilien (besonders der Squamata). *Cour. Forsch.-Inst. Senckenberg* **180**, 1–58.

Cott, H. B. (1961). Scientific results of an inquiry into the ecology and economic status of the Nile crocodile (*Crocodilus niloticus*) in Uganda and Northern Rhodesia. *Trans. Zool. Soc. Lond.* **29**, 211–340.

Currey, J. D. (1987). Evolution of the mechanical properties of amniote bone. *J. Biomech.* **20**, 1035–1044.

Currey, J. D. (1988). The effect of porosity and mineral content on the Young's modulus of elasticity of compact bone. *J. Biomech.* **21**, 131–139.

Currey, J. D. (1990). Physical characteristics affecting the tensile failure properties of compact bone. *J. Biomech.* **23**, 837–844.

Flitney, F. W. and Hirst, D. G. (1978). Cross-bridge detachment and sarcomere 'give' during stretch of active frog's muscle. *J. Physiol., Lond.* **276**, 449–465.

Gatesy, S. M. (1990). Caudofemoral musculature and the evolution of theropod locomotion. *Paleobiol.* **16**, 170–186.

Gatesy, S. M. (1991). Hind limb movements of the American alligator (*Alligator mississippiensis*) and postural grades. *J. Zool., Lond.* **224**, 577–588.

Gatesy, S. M. (1997). An electromyographic analysis of hindlimb function in *Alligator* during terrestrial locomotion. *J. Morph.* **234**, 197–212.

Harry, J. D., Ward, A., Heglund, N. C., Morgan, D. L. and McMahon, T. A. (1990). Cross-bridge cycling theories cannot explain high-speed lengthening behavior in muscle. *Biophys. J.* **57**, 201–208.

Hildebrand, M. (1976). Analysis of tetrapod gaits: general considerations and symmetrical gaits. In *Neural Control of Locomotion* (ed. R. M. Herman, S. Grillner, P. S. G. Stein and D. G. Stuart), pp. 203–236. New York: Plenum Press.

Hopson, J. A. (1991). Systematics of the nonmammalian Synapsida and implications for patterns of evolution in Synapsids. In *Origins of the Higher Groups of Tetrapods: Controversy and Consensus* (ed. H.-P. Schultze and L. Trueb), pp. 635–693. Ithaca, London: Comstock Publishing Associates.

Hopson, J. A. (1994). Synapsid evolution and the radiation of non-eutherian mammals. In *Major Features of Vertebrate Evolution, Short Course in Paleontology 7* (ed. D. R. Prothero and R. M. Schoch), pp. 190–219. Knoxville, TN: The Paleontological Society.

Hopson, J. A. (1995). Patterns of evolution in the manus and pes of non-mammalian therapsids. *J. Vert. Paleont.* **15**, 615–639.

Irschick, D. J. and Jayne, B. C. (1999). Comparative three-dimensional kinematics of the hindlimb for high-speed bipedal and quadrupedal locomotion of lizards. *J. Exp. Biol.* **202**, 1047–1065.

Irschick, D. J. and Jayne, B. C. (2000). Size matters: ontogenetic variation in the three-dimensional kinematics of steady speed locomotion in the lizard *Dipsosaurus dorsalis*. *J. Exp. Biol.* **203**, 2113–2148.

Jayes, A. S. and Alexander, R. McN. (1980). The gaits of chelonians: walking techniques for very low speeds. *J. Zool., Lond.* **191**, 353–378.

Jayne, B. C., Bennett, A. F. and Lauder, G. V. (1990). Muscle recruitment during terrestrial locomotion: how speed and temperature affect fibre type use in a lizard. *J. Exp. Biol.* **152**, 101–128.

Jayne, B. C. and Irschick, D. J. (1999). Effects of incline and speed on the three-dimensional hindlimb kinematics of a generalized iguanian lizard (*Dipsosaurus dorsalis*). *J. Exp. Biol.* **202**, 143–159.

Jenkins, F. A., Jr (1971a). Limb posture and locomotion in the Virginia opossum (*Didelphis marsupialis*) and in other non-cursorial mammals. *J. Zool., Lond.* **165**, 303–315.

Jenkins, F. A., Jr (1971b). The postcranial skeleton of African cynodonts. *Bull. Peabody Mus. Nat. Hist.* **36**, 1–216.

Jenkins, F. A., Jr and Parrington, F. R. (1976). The postcranial skeletons of the Triassic mammals *Eozostrodon*, *Megazostrodon* and *Erythrotherium*. *Phil. Trans. R. Soc. B* **273**, 387–431.

John-Alder, H. B. and Bennett, A. F. (1987). Thermal adaptations in lizard muscle function. *J. Comp. Physiol.* B **157**, 241–252.

Keller, T. S. and Spengler, D. M. (1989). Regulation of bone stress and strain in the immature and mature rat femur. *J. Biomech.* **22**, 1115–1127.

Kemp, T. S. (1980). Aspects of the structure and functional anatomy of the Middle Triassic cynodont *Luangwa*. *J. Zool., Lond.* **191**, 193–239.

Kemp, T. S. (1982). *Mammal-like Reptiles and the Origin of Mammals*. London: Academic Press.

Kemp, T. S. (1985). A functional interpretation of the transition from primitive tetrapod to mammalian locomotion. In *Principles of Construction in Fossil and Recent Reptiles* (ed. J. Reiß and E. Frey), pp. 181–191. Stuttgart: Universität Stuttgart/Universität Tübingen.

LaBarbera, M. (1989). Analyzing body size as a factor in ecology and evolution. *Annu. Rev. Ecol. Syst.* **20**, 97–117.

Landsmeer, J. M. F. (1990). Functional morphology of the hindlimb in some Lacertilia. *Eur. J. Morph.* **28**, 3–34.

Lanyon, L. E. and Rubin, C. T. (1985). Functional adaptation in skeletal structures. In *Functional Vertebrate Morphology* (ed. M. Hildebrand, D. M. Bramble, K. F. Liem and D. B. Wake), pp. 1–25. Cambridge, MA: The Belknap Press.

Lanyon, L. E. and Smith, R. N. (1970). Bone strain in the tibia during normal quadrupedal locomotion. *Acta Orthopaed. Scand.* **41**, 238–248.

Marsh, R. L. (1988). Ontogenesis of contractile properties of skeletal muscle and sprint performance in the lizard *Dipsosaurus dorsalis*. *J. Exp. Biol.* **137**, 119–139.

McArdle, B. H. (1988). The structural relationship: regression in biology. *Can. J. Zool.* **66**, 2329–2339.

Norell, M. A. and de Queiroz, K. (1991). The earliest iguanine lizard (Reptilia: Squamata) and its bearing on iguanine phylogeny. *Am. Mus. Nov.* **2997**, 1–16.

Parrish, J. M. (1987). The origin of crocodilian locomotion. *Paleobiol.* **13**, 396–414.

Peterson, J. A. and Zernicke, R. F. (1987). The geometric and mechanical properties of limb bones in the lizard, *Dipsosaurus dorsalis*. *J. Biomech.* **20**, 902.

Petren, K. and Case, T. J. (1997). A phylogenetic analysis of body size evolution and biogeography in chuckwallas (*Sauromalus*) and other iguanines. *Evolution* **51**, 206–219.

Reilly, S. M. (1994/95). Quantitative electromyography and muscle function of the hind limb during quadrupedal running in the lizard *Sceloporus clarkii*. *Zoology* **98**, 263–277.

Reilly, S. M. (1998). Sprawling locomotion in the lizard *Sceloporus clarkii*: speed modulation of motor patterns in a walking trot. *Brain Behav. Evol.* **52**, 126–138.

Reilly, S. M. and Elias, J. A. (1998). Locomotion in *Alligator mississippiensis*: kinematic effects of speed and posture and their relevance to the sprawling-to-erect paradigm. *J. Exp. Biol.* **201**, 2559–2574.

Rewcastle, S. C. (1980). Form and function in the lacertilian knee and mesotarsal joints; a contribution to the analysis of sprawling locomotion. *J. Zool., Lond.* **191**, 147–170.

Romer, A. S. (1922). The locomotor apparatus of certain primitive and mammal-like reptiles. *Bull. Am. Mus. Nat. Hist.* **46**, 517–606.

Romer, A. S. (1923). Crocodilian pelvic muscles and their avian and reptilian homologues. *Bull. Am. Mus. Nat. Hist.* **48**, 533–552.

Rubin, C. T. and Lanyon, L. E. (1982). Limb mechanics as a function of speed and gait: a study of functional strains in the radius and tibia of horse and dog. *J. Exp. Biol.* **101**, 187–211.

Rubin, C. T. and Lanyon, L. E. (1984). Dynamic strain similarity in vertebrates: an alternative to allometric limb bone scaling. *J. Theor. Biol.* **107**, 321–327.

Schaeffer, B. (1941a). The morphological and functional evolution of the tarsus in amphibians and reptiles. *Bull. Am. Mus. Nat. Hist.* **78**, 395–472.

Schaeffer, B. (1941b). The pes of *Bauria cynops* Broom. *Am. Mus. Novit.* **1103**, 1–7.

Snyder, R. C. (1954). The anatomy and function of the pelvic girdle and hindlimb in lizard locomotion. *Am. J. Anat.* **95**, 1–45.

Snyder, R. C. (1962). Adaptations for bipedal locomotion of lizards. *Am. Zool.* **2**, 191–203.

Sokal, R. R. and Rohlf, F. J. (1995). *Biometry*. Third edition. New York: W. H. Freeman & Company.

Updegraff, G. (1990). *Measurement TV: Video Analysis Software*. San Clemente, CA: Data Crunch.

Wainwright, S. A., Biggs, W. D., Currey, J. D. and Gosline, J. M. (1976). *Mechanical Design in Organisms*. Princeton: Princeton University Press.